Stem Cell Niche

1. Anatómiailag meghatározott
2. Specifikus extracell. mátrix és támogató sejtek
3. Növekedést moduláló szignálokban gazdag

Schoefield (1978) – hematopoetikus őssejtekre

Schofield's proposed features of a stem cell niche

Restriction on stem cell entry into cell cycle and differentiation programs

Integration of signals reflecting tissue and organismal state

Imposition of stem cell features on daughter cells

Mechanism for limiting "mutational errors"

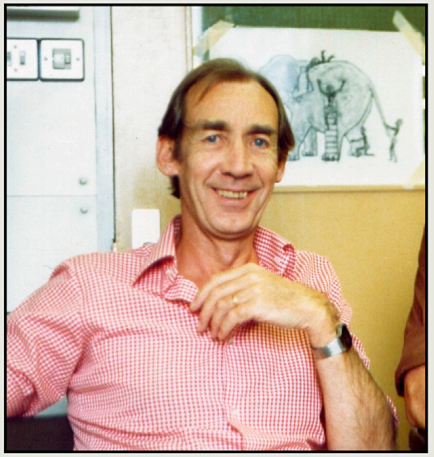

The hair follicle as a model system to study stem cells.

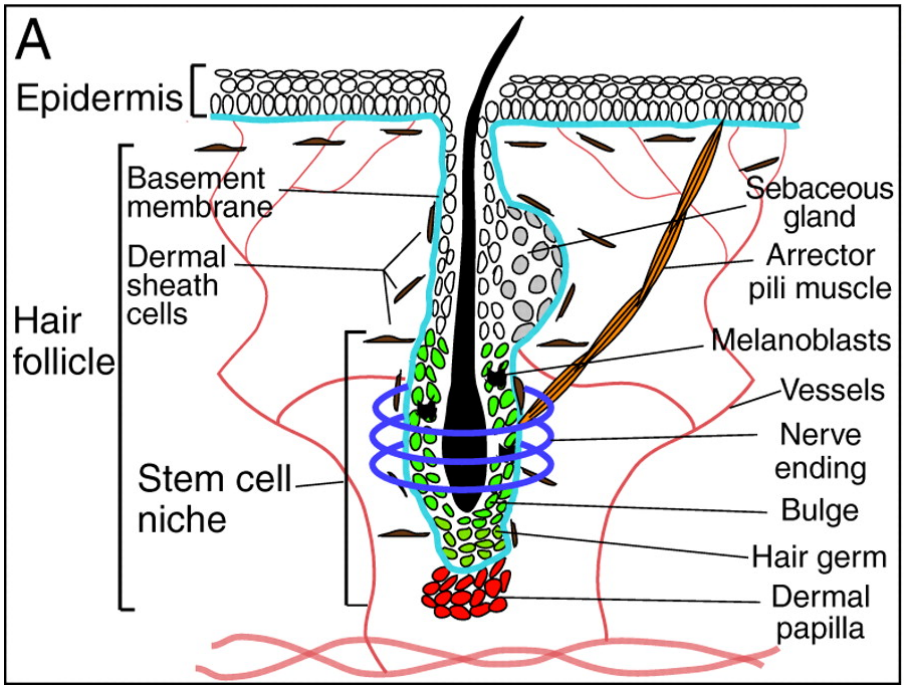

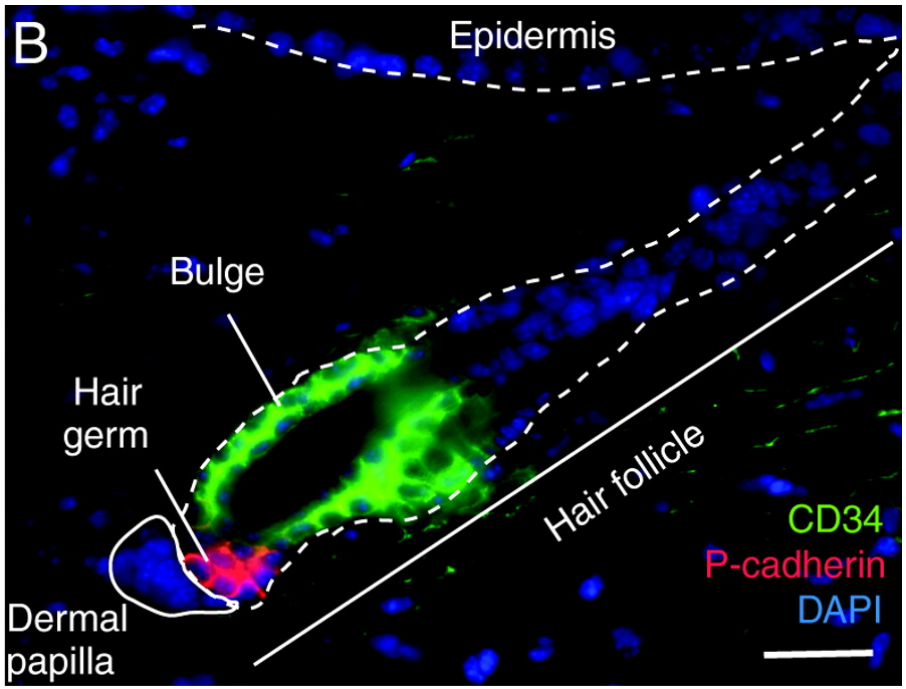

A bi-compartmental organization of different adult mammalian stem cell niches.

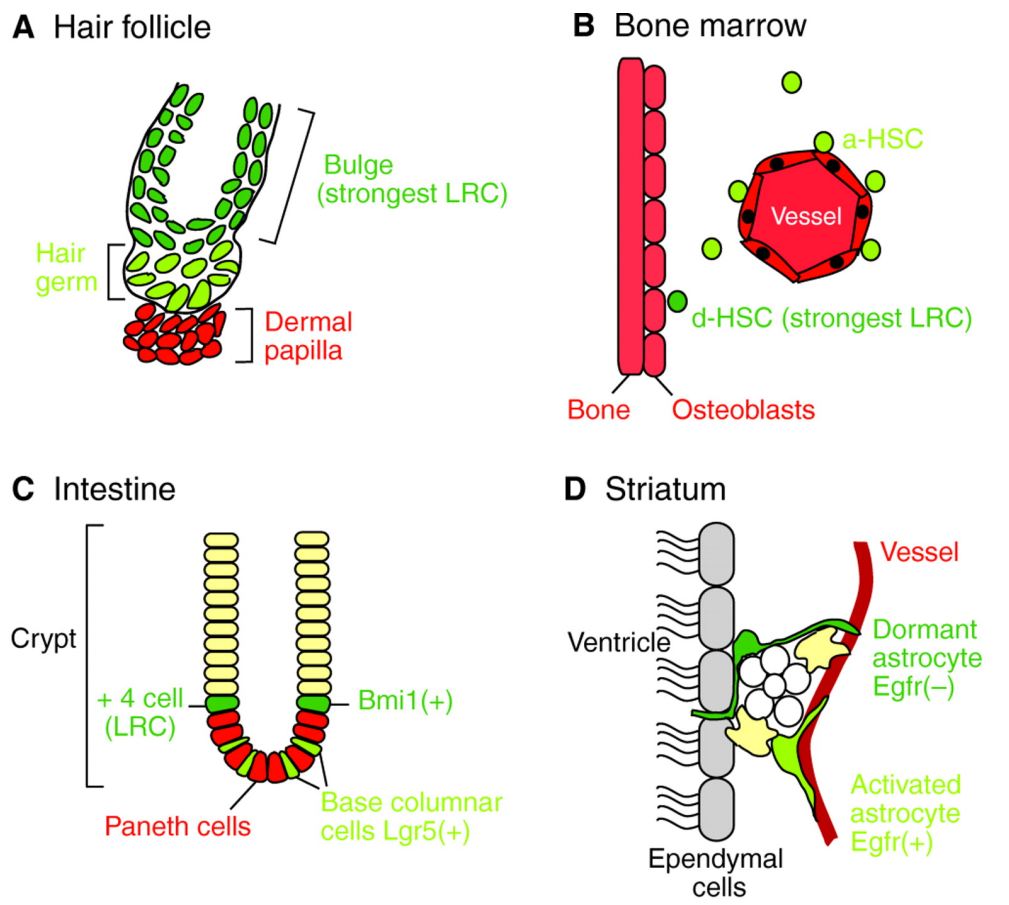

Greco V , and Guo S Development 2010;137:1586-1594

A schematic of stem cells in many tissues. Because stem cells have a slow cell cycle, they can be identified by their ability to retain nucleotide analogs such as bromodeoxyuridine (BrdU) longer than other cells, resulting in their name as label retaining cells (LRCs). (**A**) The hair follicle stem cell niche is organized into two different epithelial compartments, the hair germ and the bulge. The hair germ (light green) is located close to the mesenchymal dermal papilla (red), which acts as a signaling center. The bulge (dark green) is located further away from the dermal papilla. The cells with the most label retention are found in the bulge. (**B**) In the hematopoietic system, dormant hematopoietic stem cells (d-HSCs, dark green) and activated (a-) HSCs (light green) have been identified. The d-HSCs retain label better than do the a-HSCs and are probably located closer to the endosteal niche of osteoblasts (red), whereas the a-HSCs are probably further away from the bone and closer to the vasculature (red vessel). (**C**) In the intestine, stem cells are positive for Bmi1 (dark green) and are located in position +4 in the intestinal crypt. Lgr5-labelled stem cells (light green) have also been identified at the base of the crypts. The differentiated Paneth cells (red) could possibly function as a niche for the $Lgr5^{+}$ stem cells. (**D**) In the subventricular zone of the striatum, two groups of astrocytic stem cells have been identified: $Gfap^{+}$ $Egfr^{-}$ astrocytes (dark green) and $Gfap^{+}$ $Egfr^{+}$ astrocytes (light green). These cells presumably rely on the ventricle and the blood vessels as a niche (red). Bmi1, B lymphoma Mo-MLV insertion region 1; Egfr, epidermal growth factor receptor; Lgr5, leucine-rich repeat-containing G-protein-coupled receptor 5; LRC, label retaining cells.

Cre-recombinase-based lineage tracing system.

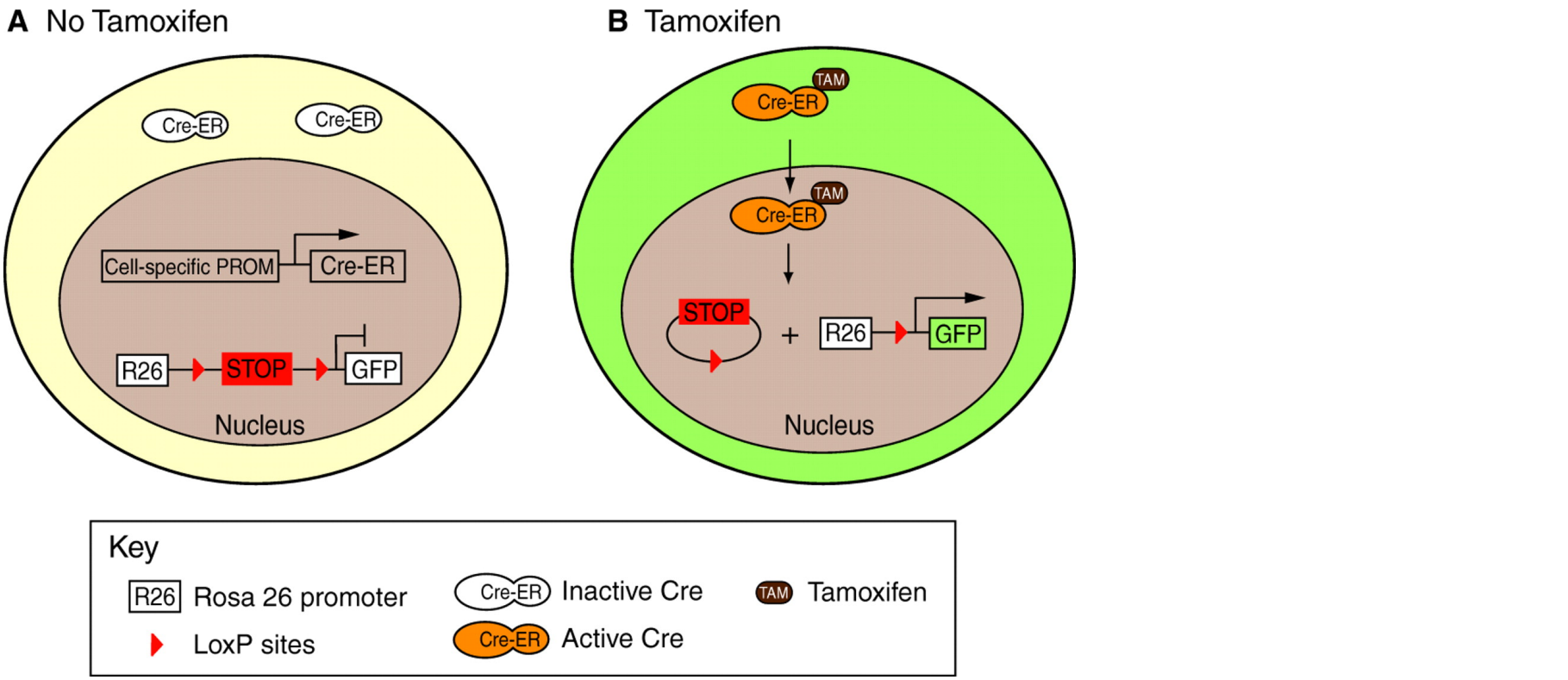

Cre-recombinase-based lineage tracing system. Cre recombinase expression can be spatially restricted by expressing it under the control of a tissue-specific promoter. Temporal restriction is achieved by fusing it to the tamoxifen-responsive hormone-binding domain of the estrogen receptor (Cre-ER^{TAM}). The Cre enzyme is in an inactive state in the absence of the ligand tamoxifen. Once tamoxifen is added, the Cre is active and can translocate to the nucleus. When these Cre constructs are used in conjunction with reporter genes, such as green fluorescent protein (GFP) ubiquitously expressed under the control of the ROSA26 (R26) promoter for example, and placed downstream of a STOP codon flanked by Cre recombinase recognition (loxP) sites, reporter gene expression can be activated in specific cell types at defined time-points. (**A**) In the absence of tamoxifen, no expression of the reporter gene is observed because of the presence of the stop signal upstream of the reporter gene. (**B**) When tamoxifen is administered, the Cre is activated and mediates recombination between the loxP sites in cells. As a consequence, the STOP codon is excised and the cells are permanently marked by the reporter gene. ER, estrogen receptor; GFP, green fluorescent protein.

Testing cell potential with lineage tracing.

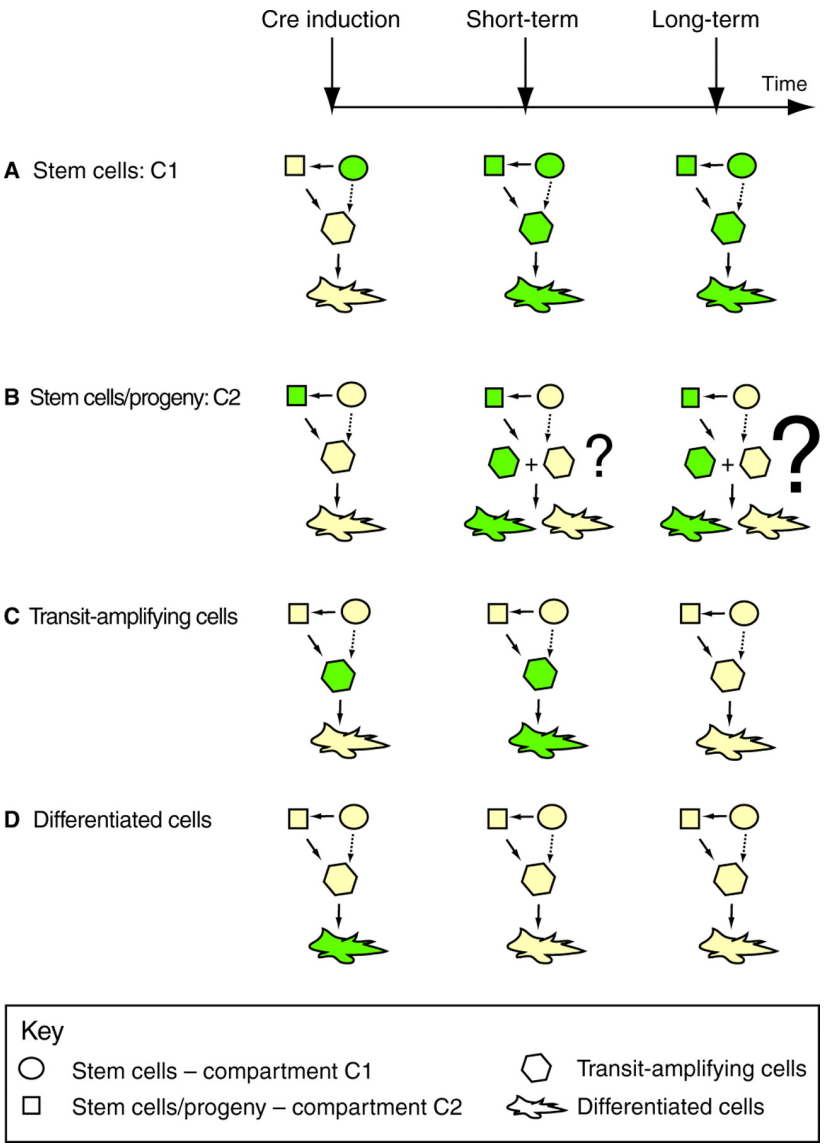

Greco V , and Guo S Development 2010;137:1586-1594

The inducible Cre system can be utilized to specifically mark different subsets of cells within a tissue. The persistence of labeled cells within a tissue is influenced by the turnover rate of the tissue, as well as by the cell cycling properties of the labeled cells. If cell-specific promoters are available (for stem cells, transit-amplifying cells or differentiated cells), several different labeling scenarios can be predicted. (**A**) If the stem cell population is marked, the whole tissue will be labeled and this label will persist for a long time, as stem cells are multipotent and long-lived. (**B**) If stem cell progeny are marked, and stem cells directly contribute to the organ regeneration, the transit-amplifying and differentiated cells will have a mosaic pattern (labeled and non-labeled cells) in the short term. If the progeny is also long-lived, this mosaic pattern will be sustained long term as well. (**C**) If transit-amplifying cells are marked, their differentiated daughter cells will also be marked in the short-term. However, as the transit-amplifying cells are short-lived, both labeled transit and differentiated cells will be replaced by unlabelled cells in the long term. (**D**) Conversely, if differentiated cells are marked, the label will be quickly lost, as differentiated cells are, in most tissues, short-lived and replaced by new stem cell progeny (there are exceptions of long-lived differentiated cells, such as memory B and T cells). By using this scheme, it is possible to address the regenerative potential of each of the cellular compartments without disrupting normal tissue physiology.

A gasztro-intesztinális rendszer fejlődése

AIP: Anterior intestinal portal
CIP: Caudal intestinal portal

Sonic hedgehog (Shh) termelés

Mezodermális Bmp-4 termelés indukálása

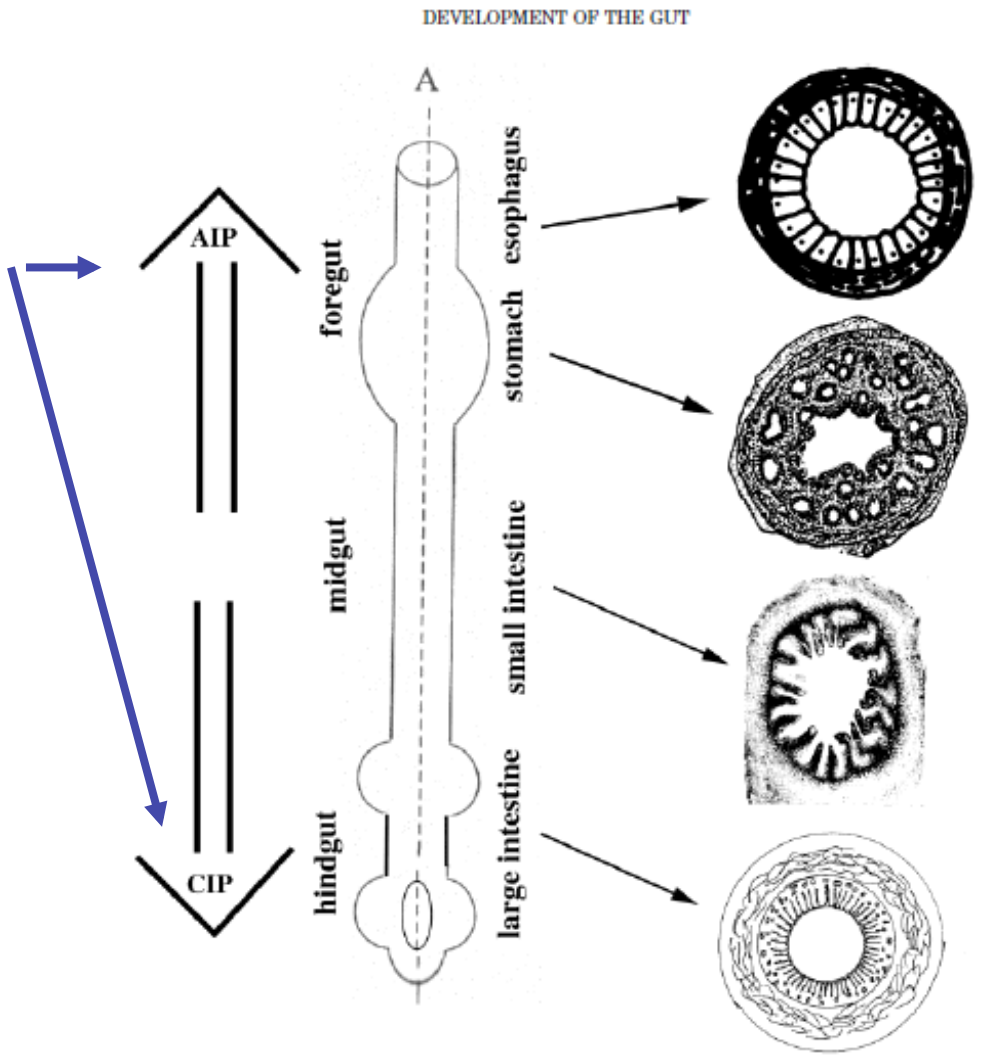

Fig. 2. Anterior-posterior (AP) pattern development in the gut. The left diagram shows the anterior intestinal portal (AIP) and caudal intestinal portal (CIP) and opposite poles of the embryo. The middle figure shows early AP regionalization into foregut, midgut, and hindgut with near adult epithelial (radial) differentiation of specific regions shown on right.

Az emésztőrendszer tagolódását szabályozó faktorok csirkében

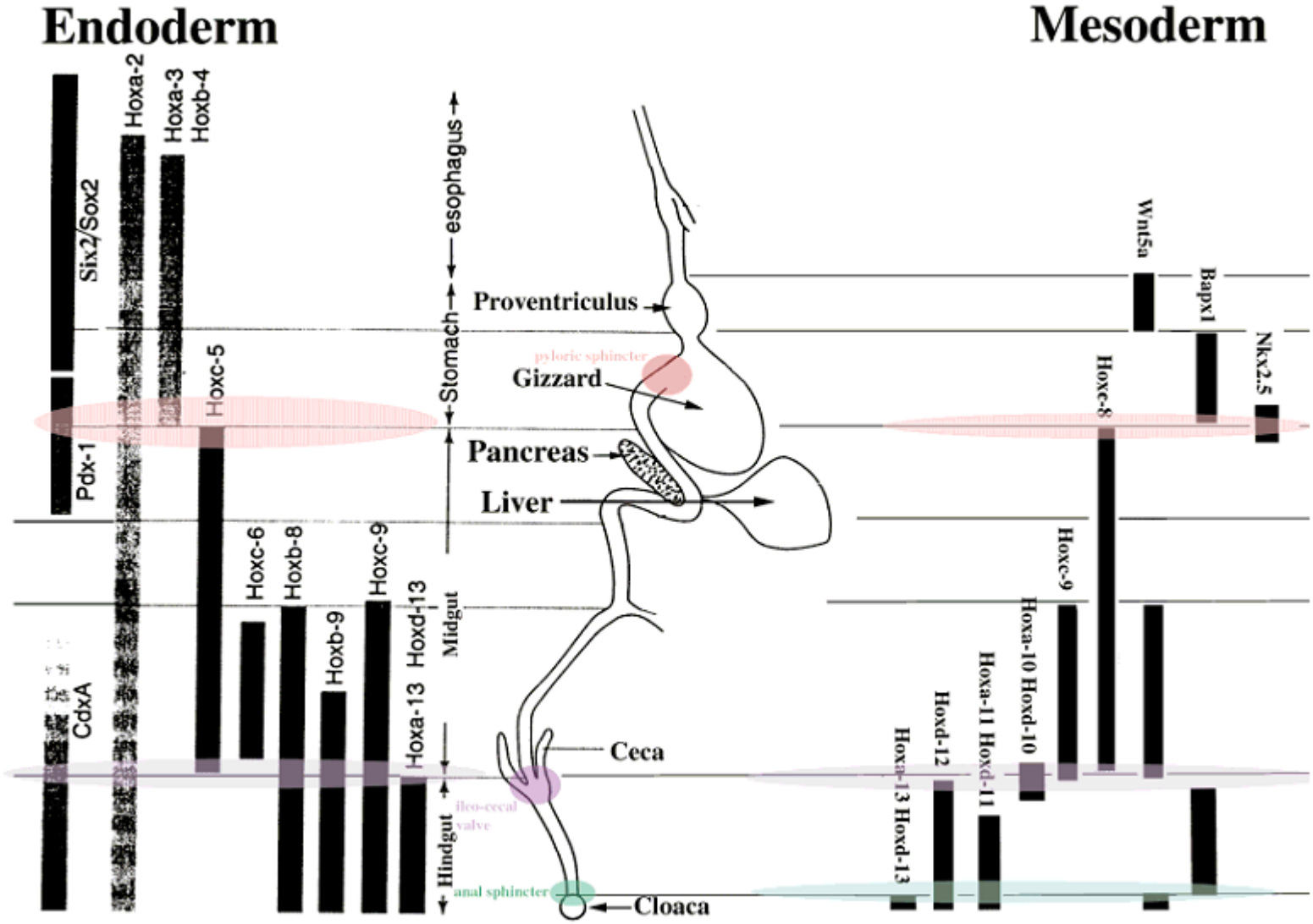

Fig. 4. Expression boundaries of selected factors in the endoderm and mesoderm with specific reference to sphincter placement. (Adapted from Grapin-Botton and Melton, 2000).

A bélhám fejlődése emlősökben

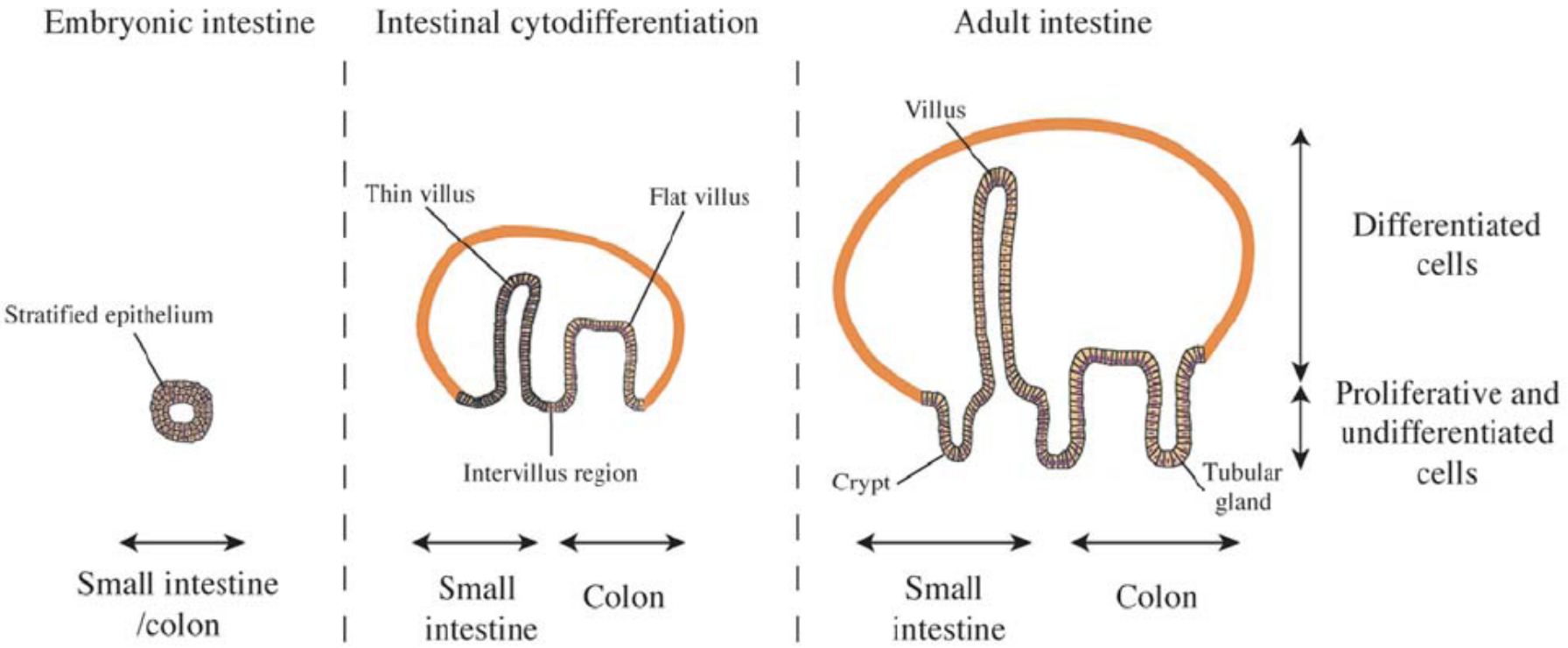

Figure 1. From development to differentiation of the intestinal epithelium. During early embryonic development, the visceral endoderm appears uniform and presents stratified cell layers. Intestinal epithelial cytodifferentiation occurs during fetal development and is marked by mesodermal growth into the lumen, and villi formation. These villi are separated by proliferative intervillus epithelium. AP axis differences appear and are characterized by long and thin villi in the small intestine and by transitory wide and flat villi in the colon. The intervillus epithelium of the small intestine is reshaped downward forming crypts. In humans, the final architecture of the small intestine is reached before birth and is characterized by the crypt-villus unit. The colonic villi disappear at the time of birth and the mature colonic epithelium presents tubular glands (crypts) [adapted from ref. 111, fig. 2].

A felnőtt bélhám szerkezete

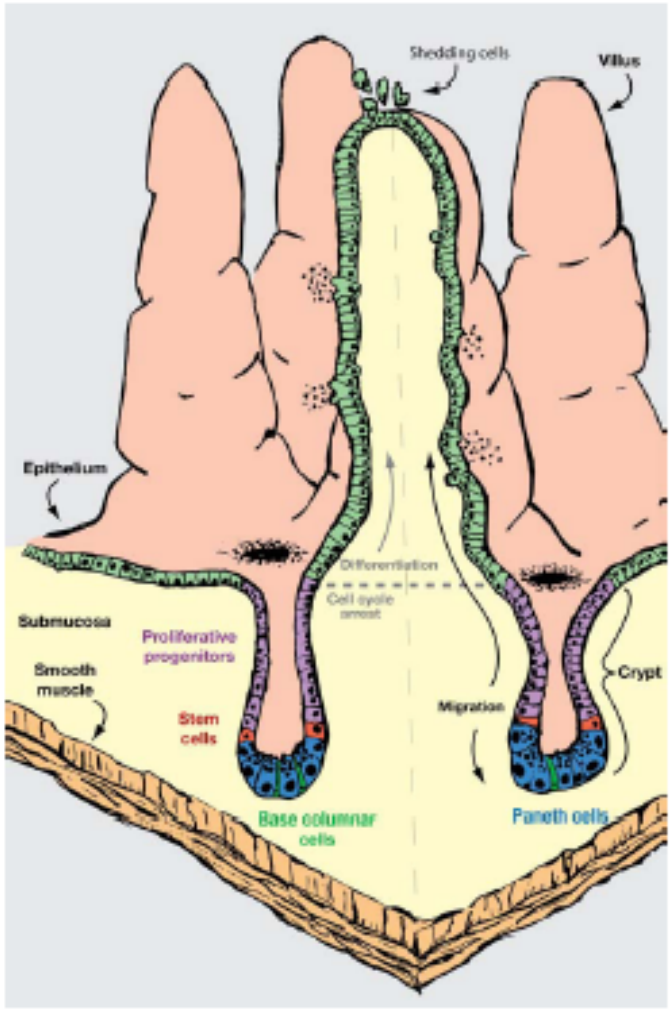

Figure 1 The structure of the adult small intestine. Putative stem cells reside immediately above the Paneth cells. Base columnar cells, intermingled between the Paneth cells, may also behave as stem cells. Progenitors stop proliferating at the crypt-villus junction and express differentiation markers. Enteroendocrine, absorptive, and mucose-creting cells migrate upward, whereas Paneth cells migrate downward and localize at the bottom of the crypts.

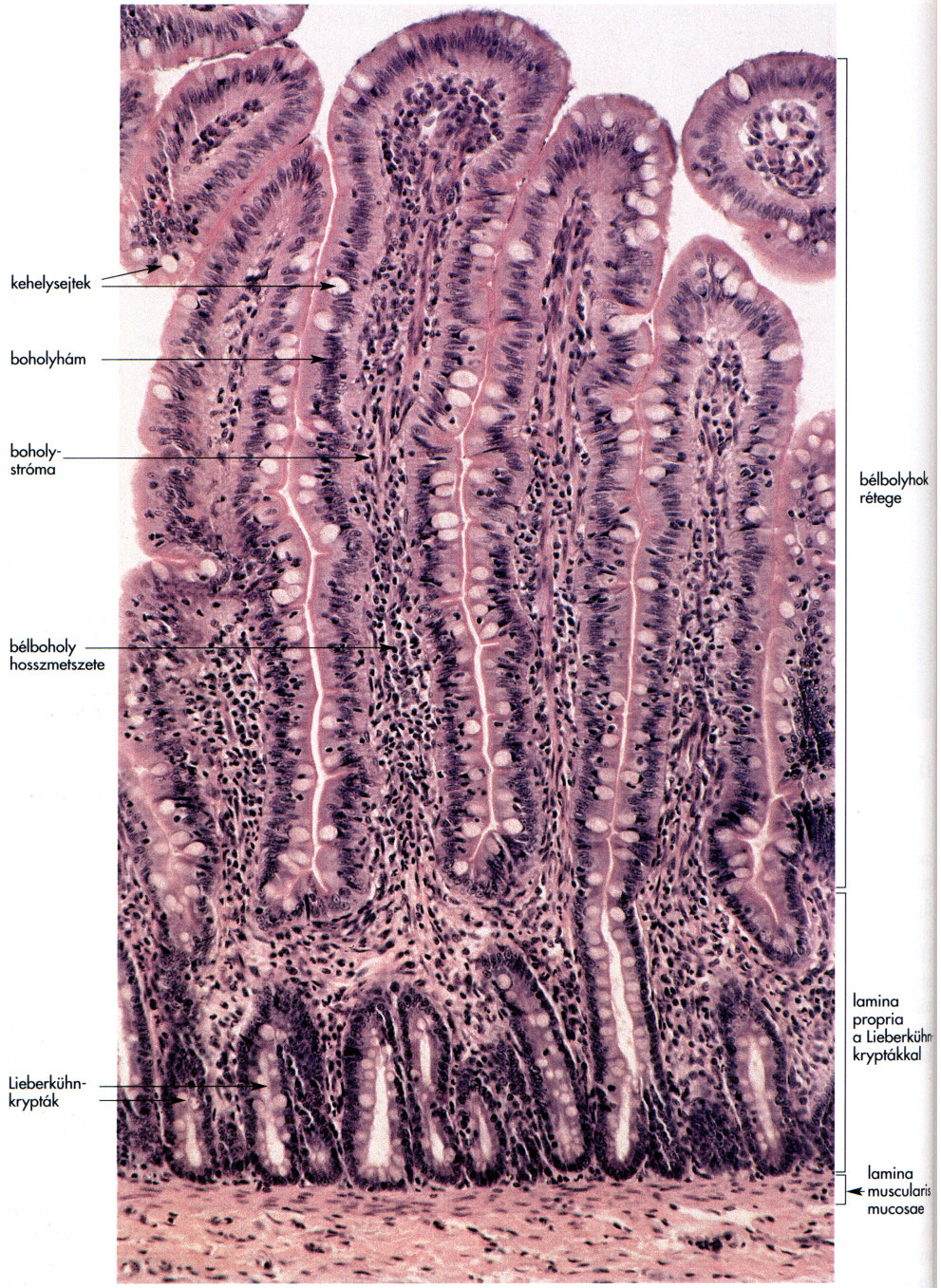

13-31. ábra. Jejunum nyálkahártyája (HE, 270x).

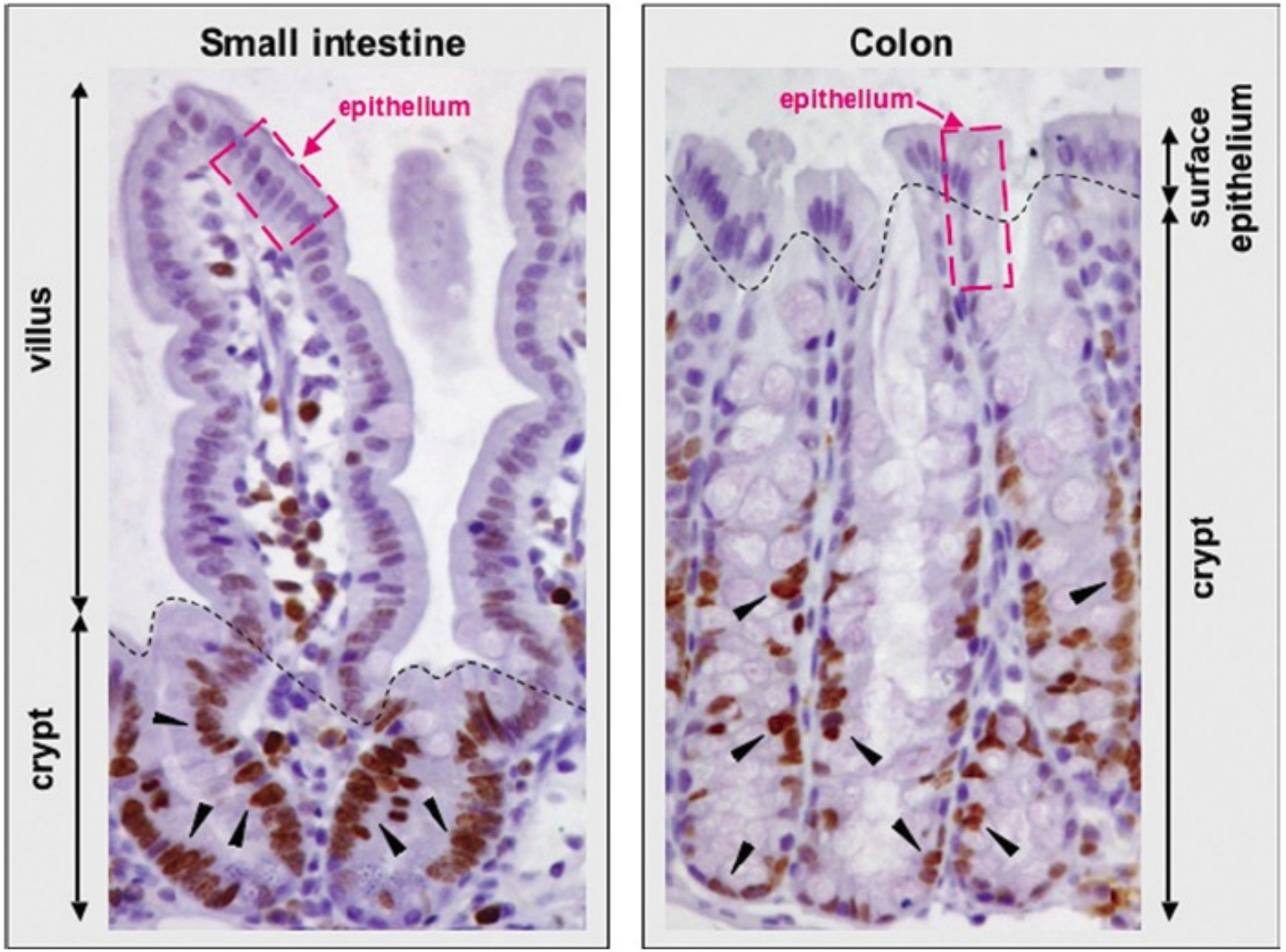
Small intestine
epithelium
villus
crypt
Colon
epithelium
surface epithelium
crypt

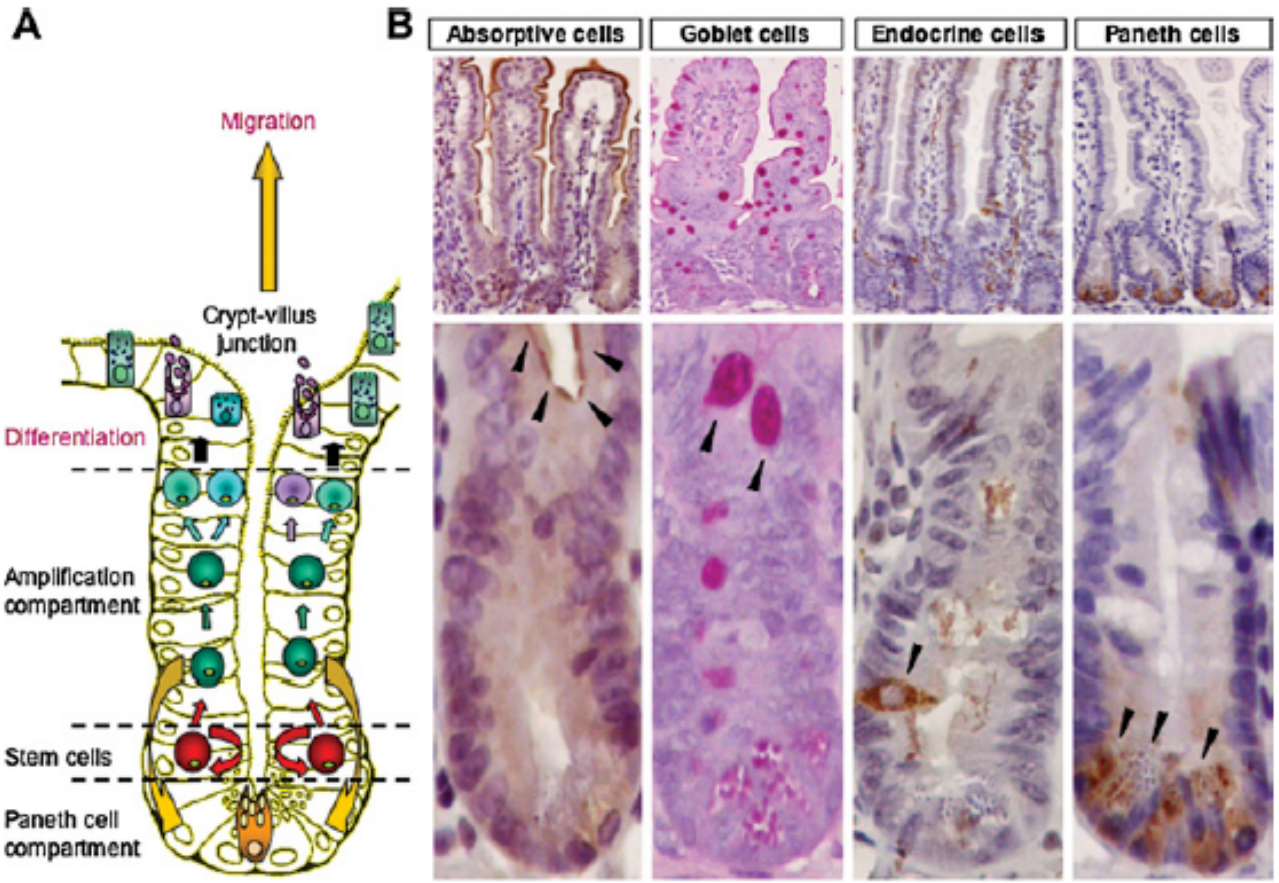

A nyálkahártya (lamina epithelialis) főbb sejttípusai:

4-5 nap alatt cserélődnek

1. enterociták: felszívóhám
2. kehelysejtek: mucin termelés a nyálkahártya védelmére
3. enteroendokrin sejtek: peptid hormon termelés
4. Paneth sejtek: a baktérium flóra „karbantartása”

Gastrointestinalis epithelium

Akkor mégis melyik az őssejt? ⇨
^{3}H-timidin, BrdU-inkorporációs vizsgálatok

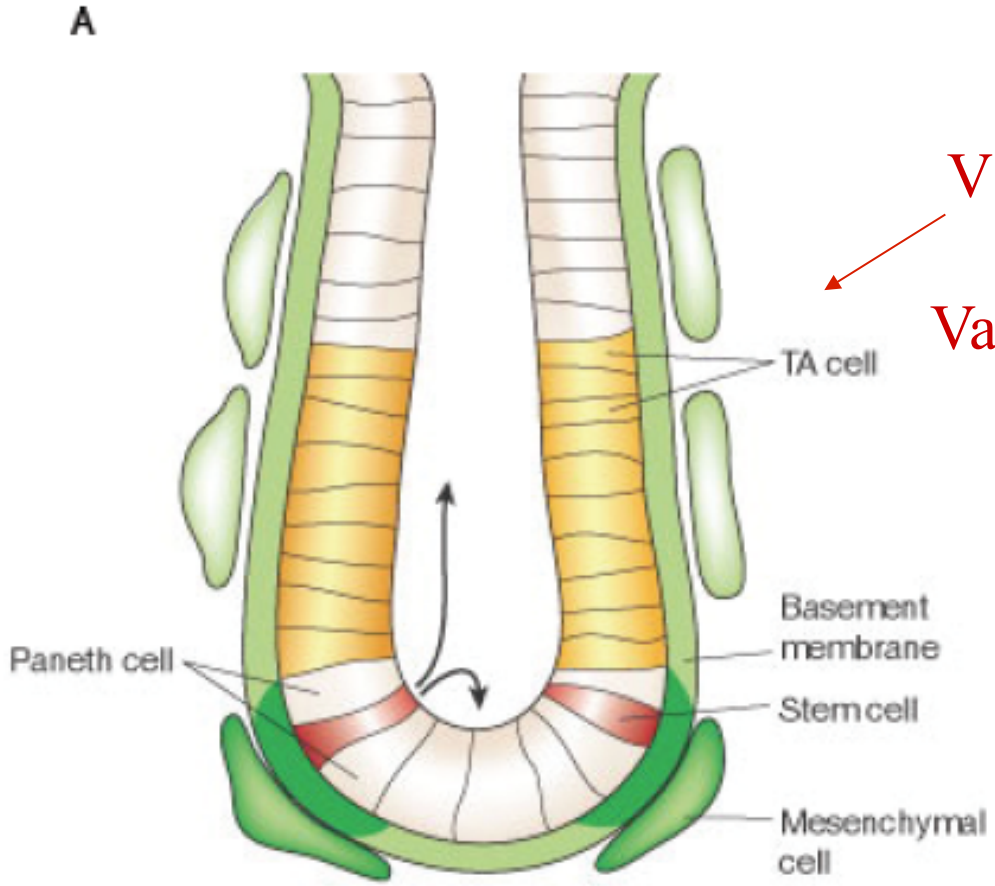

Vékonybél: Paneth-sejtek felett

Vastagbél: kripta közepén (colon ascendens.),
illetve alján (colon desc.),

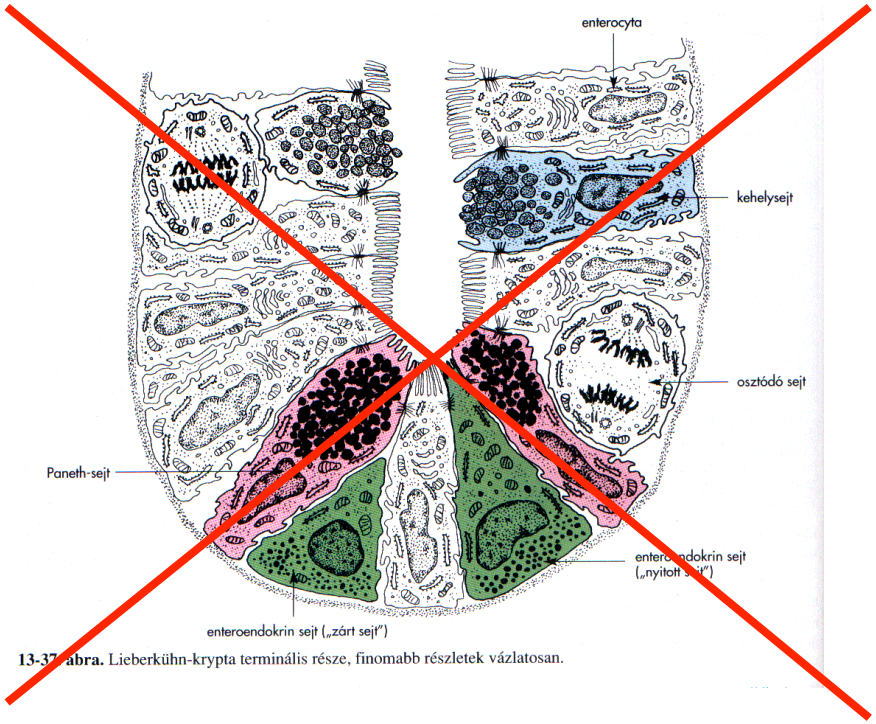

13-37. ábra. Lieberkühn-krypta terminális része, finomabb részletek vázlatosan.

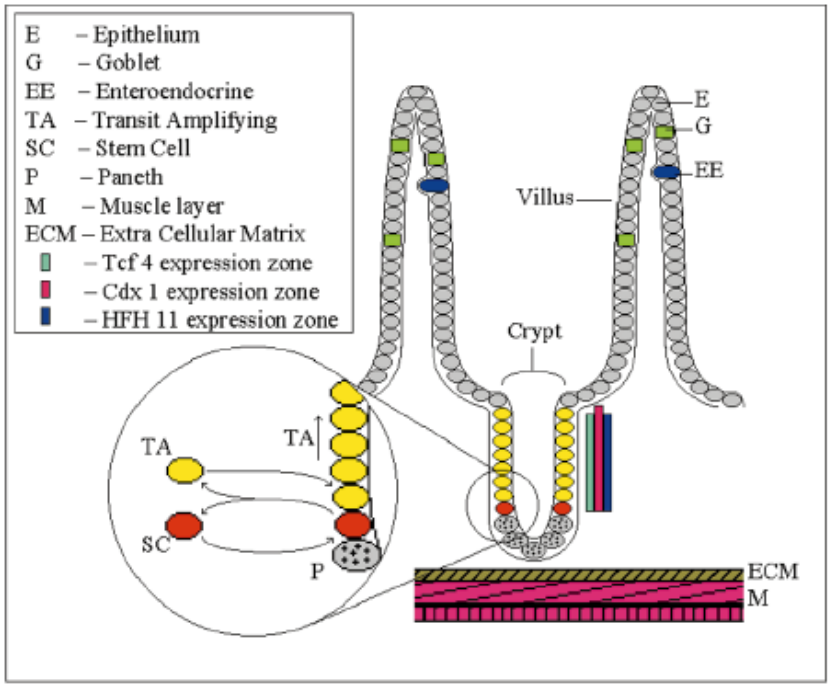

Fig. 1. Schematic representation of a section through the mammalian small intestine along the crypt villus axis indicating the location of the various cell types and the transit and stem cells. A section of the crypt region is enlarged to show the relationship between the stem and TA cells in terms of proliferation. Vertical arrows indicate direction of cell migration and differentiation. Expression domains of *Tcf-4*, *Cdx1*, *Cdx2* and *HFH11* are also indicated.

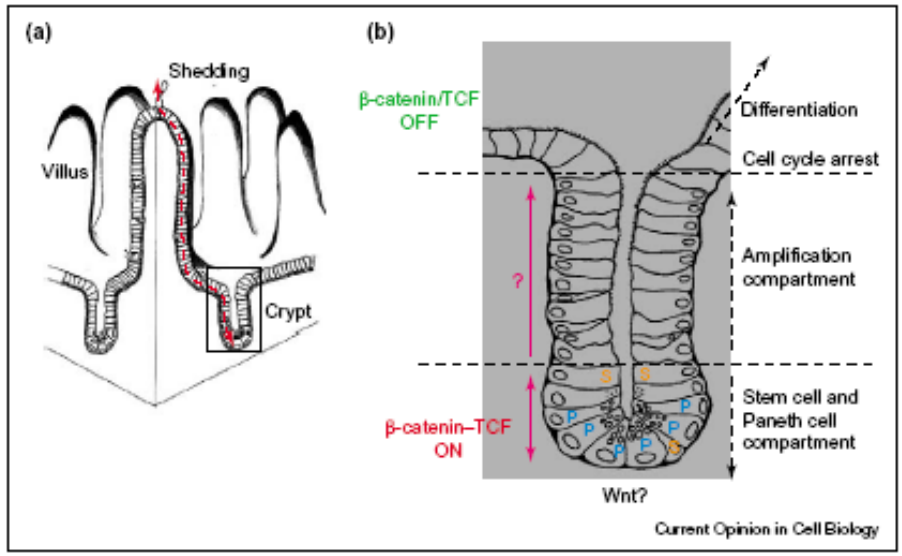

Gastrointestinalis epithelium

És mennyi van belőlük?

„unitáriánus hipotézis”: Egy őssejt képes létrehozni egy teljes kriptát. **Kripta: klonális?**

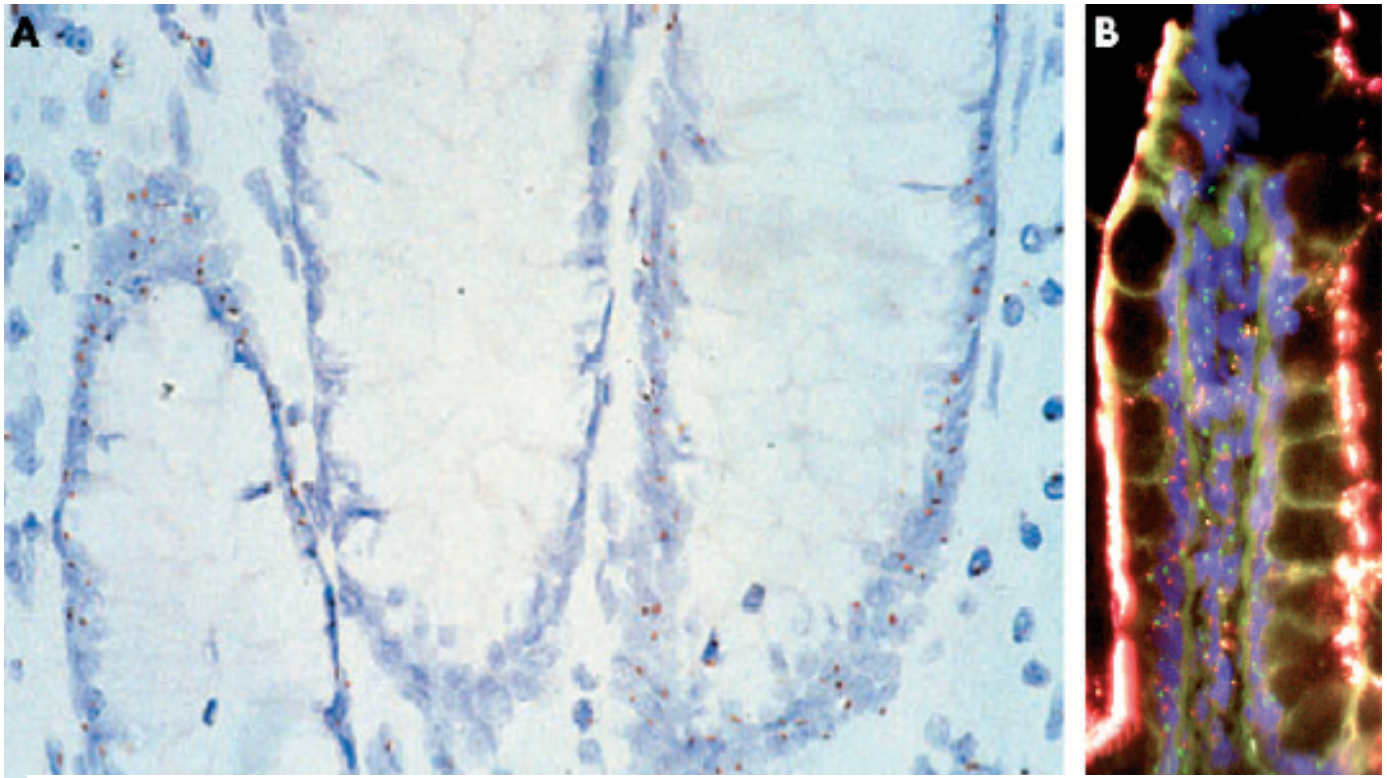

Figure 1 Clonal origin of normal human intestinal crypts and small intestinal villi. (A) Monoclonal origin of human colonic crypts: normal colonic mucosa in an XO/XY mosaic individual stained by in situ hybridisation for a Y chromosome specific probe showing a XO crypt (central) surrounded by two XY crypts (courtesy of M Novelli). (B) Villi, receiving cells from more than one crypt of different clonal derivation, show a polyclonal pattern in this X0/XY patient. Apart from the occasional Y chromosome positive inflammatory cell (red chromosome label) the majority of cells on the right of this villus are XO (green chromosome paint) whereas on the left side the cells are XY (red and green chromosome paint) (courtesy of R Poulsom).

Kísérletek besugárzott kiméra egerekkel (XX/XY), illetve ritka emberi fenotípusok: X0/XY

A Lieberkühn kripták egysejt eredetűek?

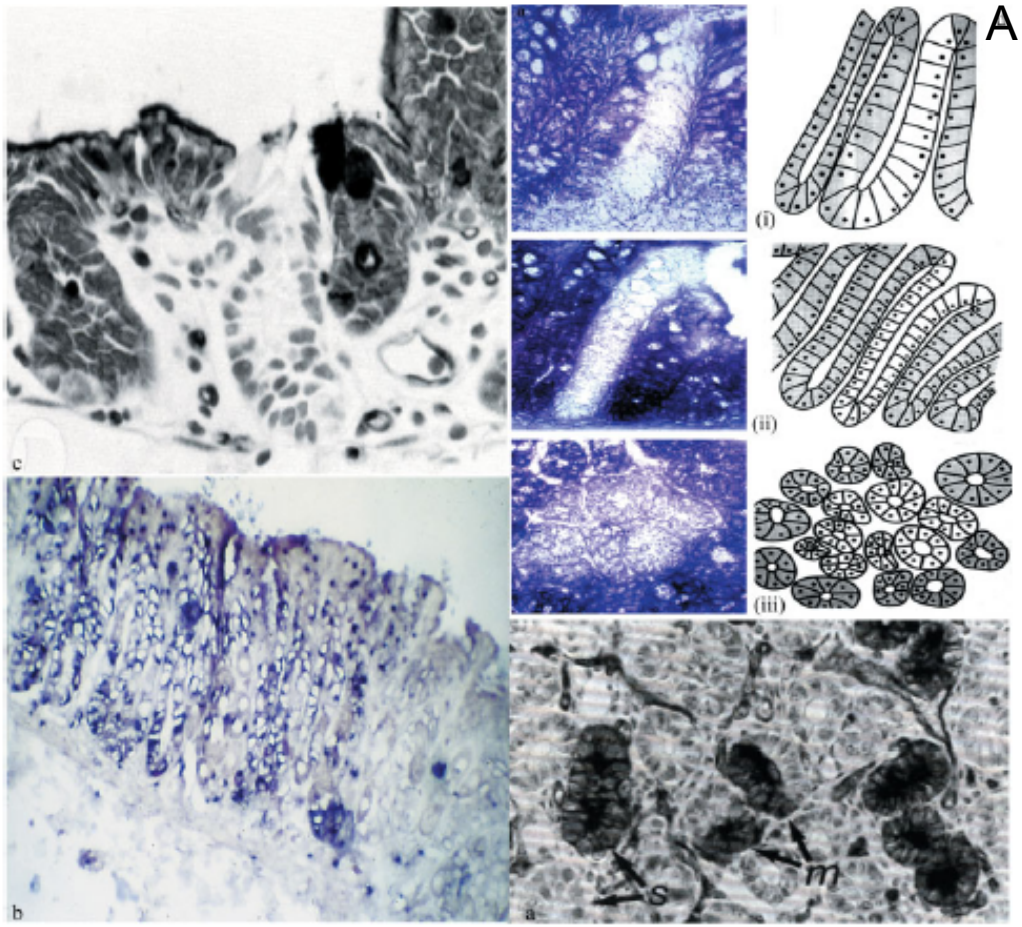

Figure 1. Mouse embryo aggregation chimeras, XX/XY chimeric mice, and X-inactivation mice in gastrointestinal clonality studies. (a) Cross-section through crypts in neonatal duodenum of a B6-SWR chimera stained with DBA (B6 = black staining; SWR = unstained). A balanced contribution to mixed crypts (m) and monoclonal crypts (s) is seen (from ref. 16, with permission). (b) Y-spot pattern in the gastric mucosa and underlying tissues of an XX–XY chimera (courtesy of E. M. Thompson). (c) DBA staining patterns in small intestine of ENU-treated (12 weeks) C57BL/6J-SWR F1 chimeras showing wholly negative and positive (black staining) crypts (from ref. 20, with permission). (d) G6PD histochemistry in frozen sections of colonic mucosa in an ENU-treated C3H mouse: (i) partially negative crypt; (ii) completely negative crypt; (iii) cross-section of an eight-crypt patch at 21 weeks (from ref. 26, with permission)

1, Embrió aggregációs kísérletek: C57Bl/6xSWR egerekben a DBA (Dolichos biflorus agglutinin) kötődés vizsgálata ⇒ csak monoklonális kripta

2, XX/XY kimérák vizsgálata

3, X inaktivációs vizsgálatok: kezdetben poliklonális, majd monoklonálissá válik

probléma:monotipikusak vagy monoklonálisak a kripták?

4, Őssejt mutációs kísérletek (besugárzás, DMH, ENU mutagenezis):

- Dlb-1 analízis: DBA kötés vizsgálja
- X inaktivációs kísérletek: $G6PD^{+/-}$

Gastrointestinalis epithelium

G6PD „mediterrán” mutációja (szardíniai nők 17%-a heterozigóta):
2260 kriptát megvizsgálva nem találtak vegyes fenotípusút:

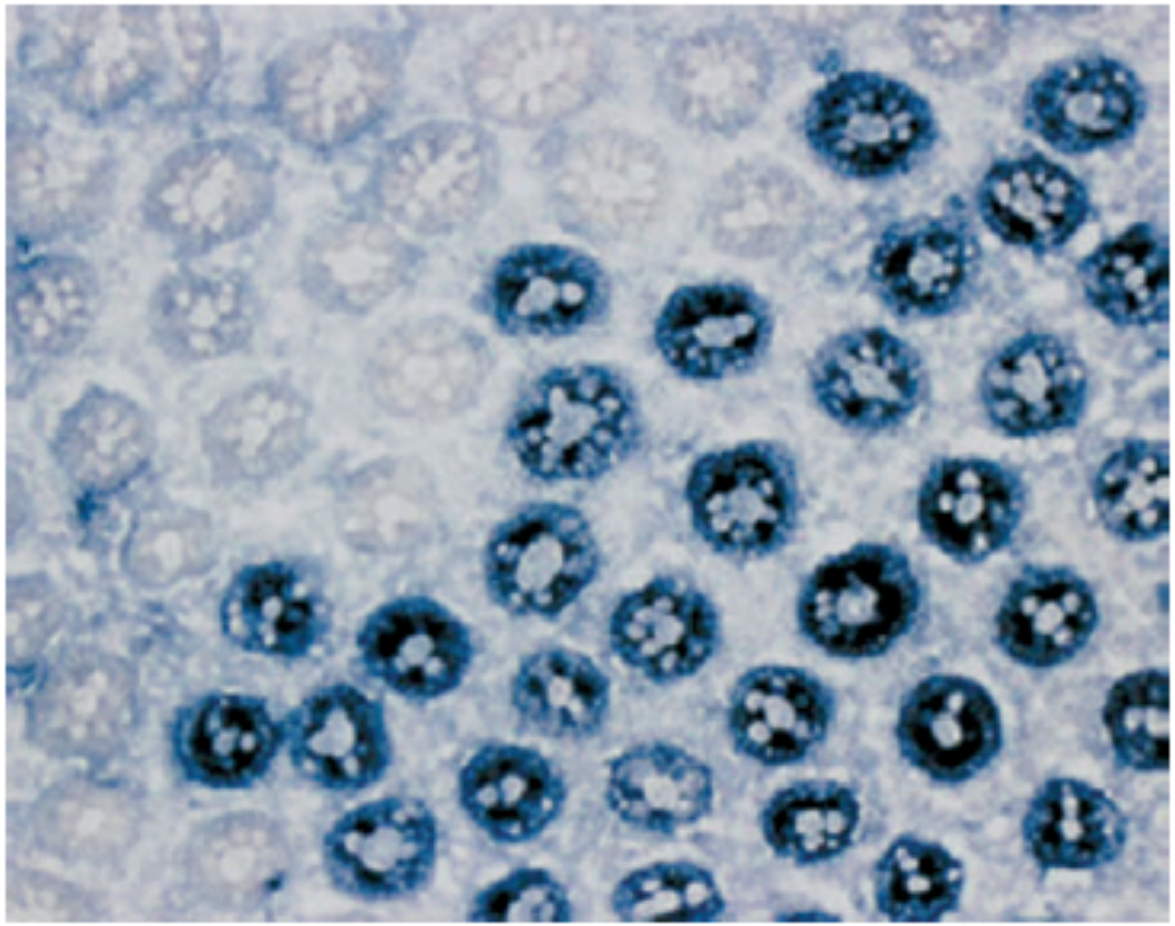

Kripták valóban monoklonálisak

A kriptá k lefűződése

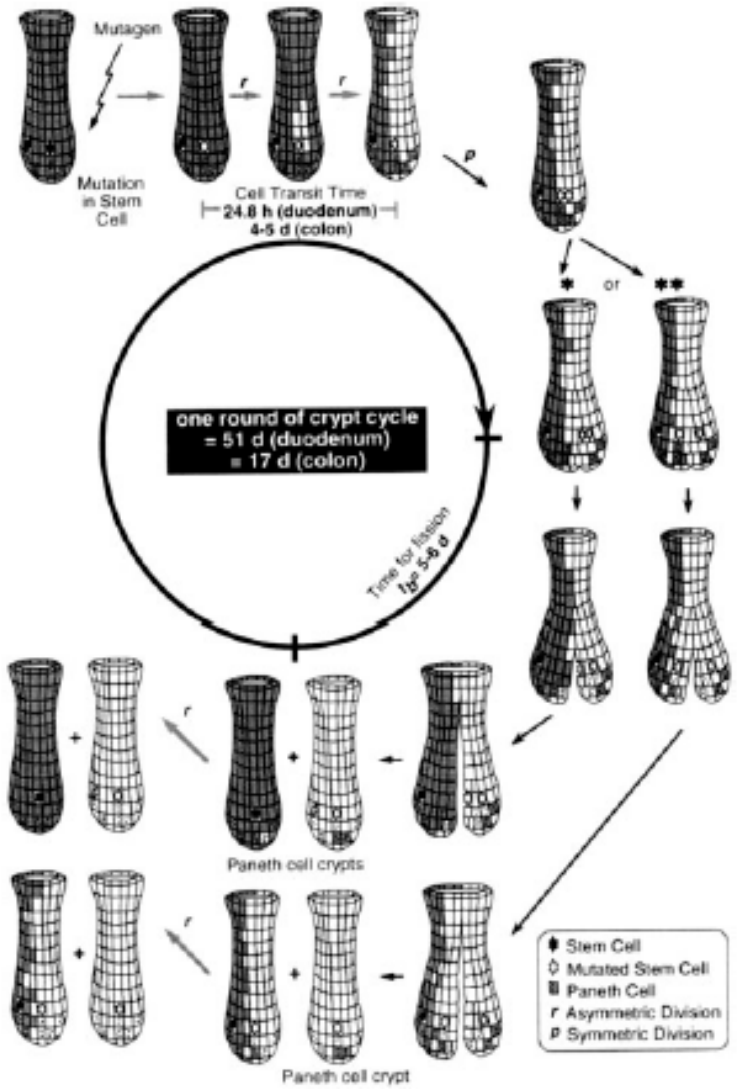

Figure 3. The crypt cycle. Emergence of transformed crypts after mutation in a single stem cell. Solid black arrows indicate the crypt division cycle, triggered by symmetric stem cell divisions (p), whereas paler arrows show asymmetric stem cell divisions (r). This is independent of the crypt cycle and enables individual crypts to maintain a constant number of stem cells and to replace differentiated progeny continuously over a crypt cell turnover time, on average (from ref. 26, with permission)

Több őssejt létezik: 4-6 db / kripta

Humán mintákon végzett DNS metiláltságot elemző vizsgálatok is hasonló eredményre jutottak

Új őssejtmarker: Lgr5

orphan G fehérje kapcsolt receptor

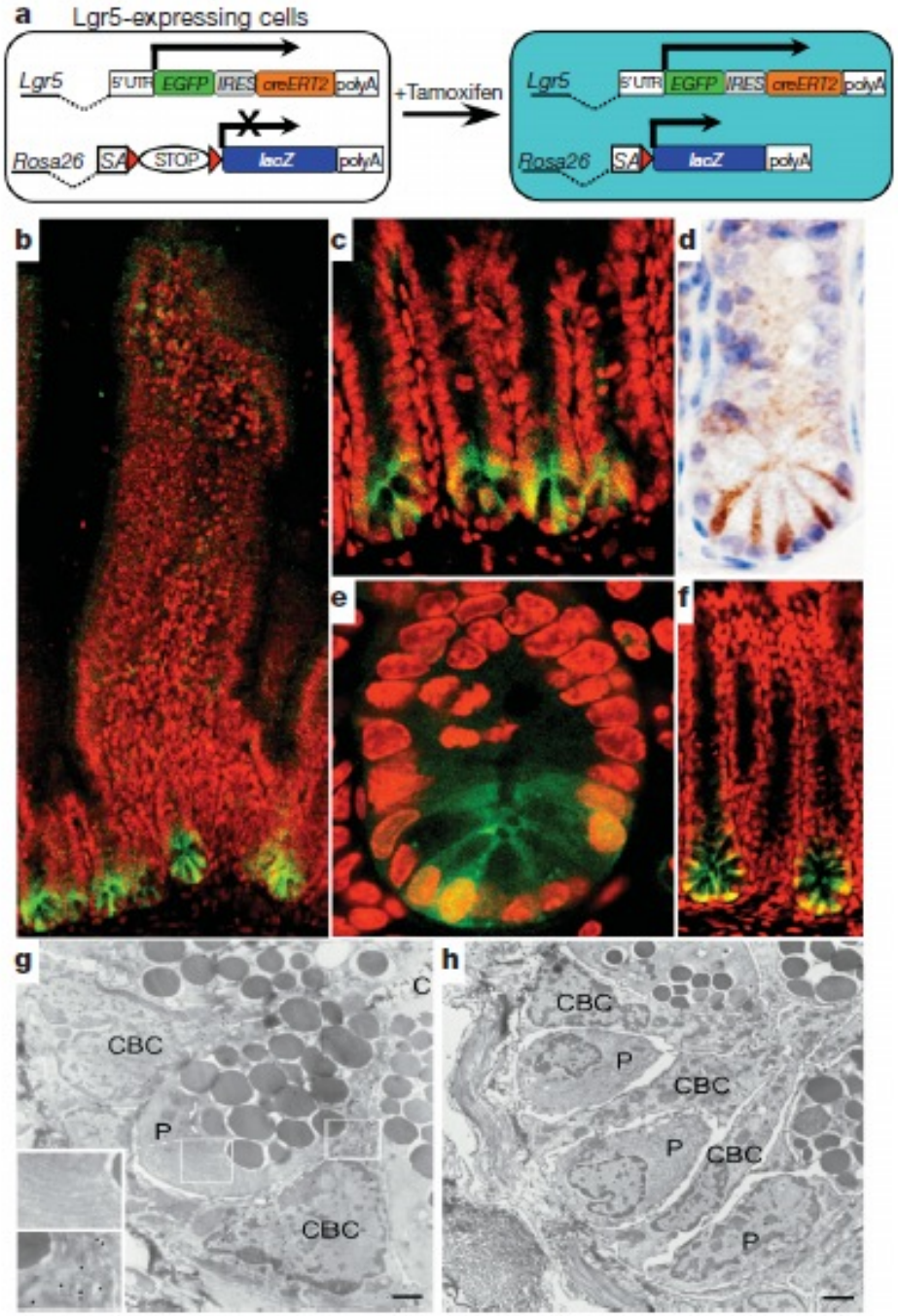

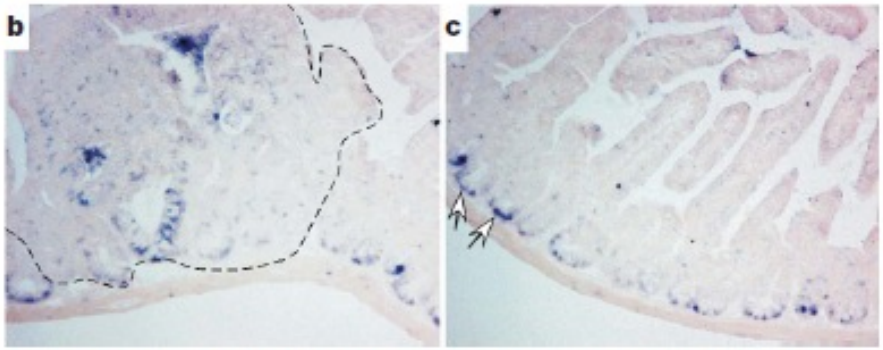

Figure 1 | *Lgr5* is a Wnt target gene in a human colon cancer cell line and is expressed in mouse crypts. **a**, Northern blot analysis (upper panel);

Figure 4 | EGFP expression in an *Lgr5-EGFP-IRES-creERT2* knock-in mouse faithfully reproduces the *Lgr5-lacZ* expression pattern in the intestinal tract. **a**, Generation of mice expressing EGFP and *creERT2* from a single bicistronic message by gene knock-in into the first exon of *Lgr5*. SA, splice acceptor; UTR, untranslated region. **b**, **c**, **e**, Confocal GFP imaging counter-stained with the red DNA dye ToPro-3 confirms that *Lgr5* expression is restricted to the six to eight slender cells sandwiched between the Paneth cells at the crypt base of the small intestine. **b**, The entire crypt–villus unit; **c**, enlargement of crypt regions; **d**, immunohistochemical analysis of EGFP expression in intestinal crypts. **e**, Two-dimensional image of three-dimensional reconstruction (Supplementary Movie 1 and Supplementary Fig. 2). **f**, Confocal imaging of EGFP expression in the colon confirms that *Lgr5* expression is restricted to a few cells located at the crypt base. **g**, Cryo-electron microscopy section of crypt stained for GFP with immunogold (scale bar, 1,000 nm). Quantification of specificity of labelling: gold particles were counted over 255 μm^2 of CBC cell cytosol (1,113 particles), 261 μm^2 of Paneth cell cytosol (305 particles) and 257 μm^2 of fibroblast cytosol (263 particles) outside the crypt. Thus, CBC cytoplasm had 4.36 gold particles per μm^2; in contrast, the Paneth cells had 1.17 gold particles per μm^2 and the fibroblast control had 1.02 gold particles per μm^2. C, crypt lumen; P, Paneth cells. **h**, Unlabelled cryo-electron microscopy section (scale bar, 2,000 nm), underscoring the ultrastructural characteristics of CBC cells and their positions relative to Paneth cells.

Több különböző őssejt létezik?

1. +4 sejtek
2. CBC (crypt based cells)

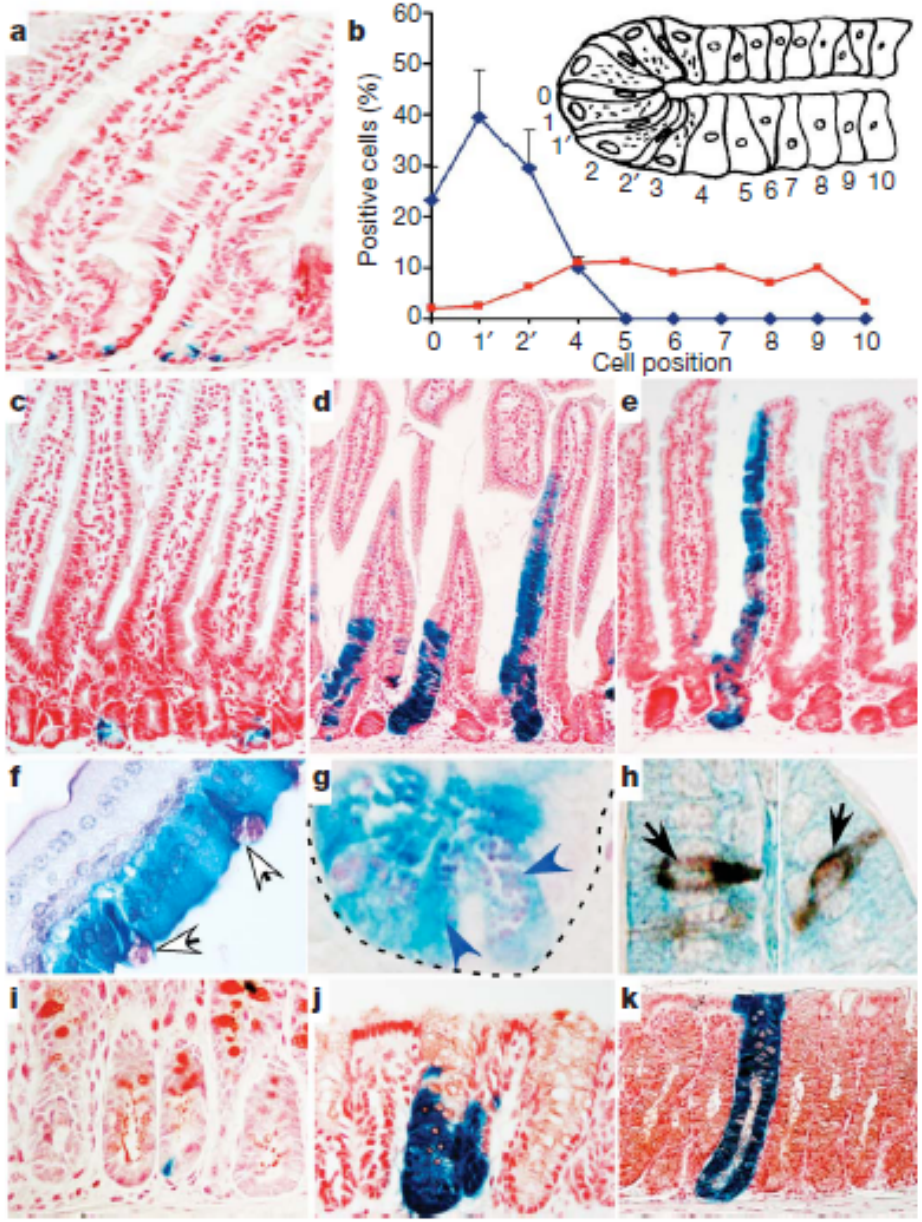

Figure 5 | Lineage tracing in the small intestine and colon. **a**, *Lgr5-EGFP-IRES-creERT2* knock-in mouse crossed with *Rosa26-lacZ* reporter mice 12 h after tamoxifen injection. **b**, Frequency at which the blue cells appeared at specific positions relative to the crypt bottom, according to the scheme in the inset. Results are depicted as means and standard deviations of four independent stretches of proximal small intestine totalling 400 positive crypts. Most of the Cre^+ LacZ-labelled CBC cells occurred at positions between the Paneth cells, whereas only 10% of these cells were observed at the +4 position directly above the cells (blue line). Quantitative data on the position of long-term DNA-label-retaining cells obtained in adult mice after irradiation (marking the '+4' intestinal stem cell) were published recently[17]. The graph shows a comparison of these data (red line) with the position of CBC cells carrying activated Cre. **c**–**e**, Histological analysis of LacZ activity in small intestine 1 day after induction (**c**), 5 days after induction (**d**) and 60 days after induction (**e**). **f**–**h**, Double-labelling of LacZ-stained intestine using PAS demonstrates the presence of goblet cells (**f**, white arrows) and Paneth cells (**g**, blue arrows) in induced blue clones. Double-labelling with synaptophysin demonstrates the presence of enteroendocrine cells within the induced blue clones (**h**, black arrows). **i**–**k**, Histological analysis of LacZ activity in colon 1 day after induction (**i**), 5 days after induction (**j**) and 60 days after induction (**k**).

Őssejt niche

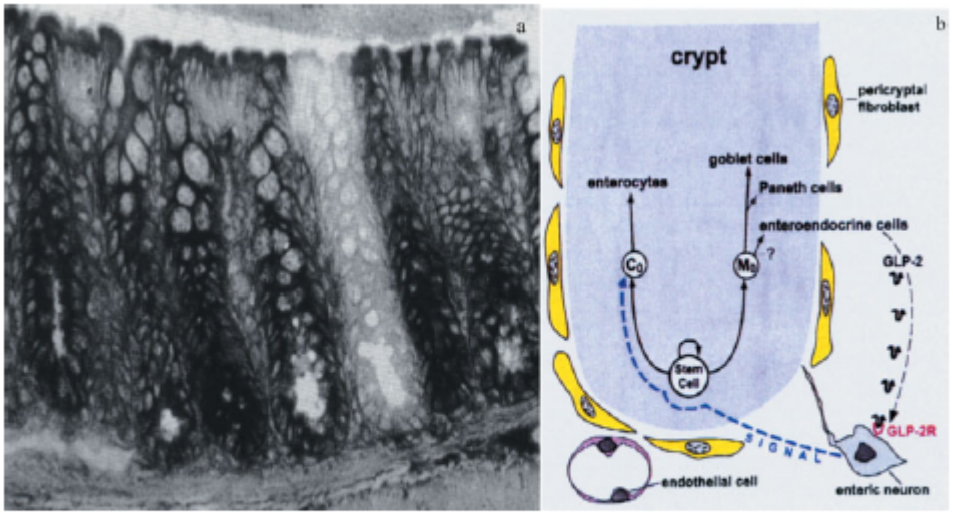

Figure 2. The stem cell niche hypothesis. (a) G6PD-stained frozen section of colonic mucosa from a CH3 mouse 14 days after a single dose of DMH showing a single wholly mutated crypt in which all cells have been replaced by a mutant phenotype (from ref. 25, with permission). (b) Diagrammatic representation of the stem cell niche. An active multipotent stem cell (SC) produces a daughter cell (C_o) that gives rise to enterocytic lineages, and another which generates goblet, Paneth, and enteroendocrine cells (although it is not known whether all derive from M_o). GLP-2 produced by a subset of enteroendocrine cells stimulates proliferation of the C_o daughter via an interaction with enteric nervous system neurons that express the GLP-2 receptor (GLP-2R). The nature of the neuronal signal that affects C_o is unknown (from ref. 100 with permission)

A speciális mikrokörnyezet meghatározó elemei:

- •Wnt szignalizáció
- •FGF, EGF, TGFb, IGF-1,2
- •PDGFa
- •Shh, Ihh
- •ISEMF sejtek? (Fhk-6⇒HSPGs-Wnt/b-catenin)

TABLE 1 Markers of cell type or compartment in the intestinal epithelium

	Cell type	References (*)
Proliferative		
Ki67	All proliferative cells	(van de Wetering et al. 2002)
c-Myc	Proliferative—mainly bottom two thirds of crypts	(Pinto et al. 2003)
NRP-B	All proliferative crypt cells	(van de Wetering et al. 2002)
CD44	All proliferative crypt cells	(van de Wetering et al. 2002)
SHH	Intervillus pockets in fetal small intestine	(Ramalho-Santos et al. 2000)
IHH	Intervillus pockets in fetal small intestine	(Ramalho-Santos et al. 2000)
Musashi-1	Stem cells + base columnar cells	(Nishimura et al. 2003)
EphB3	Stem cells + base columnar cells	(Batlle et al. 2002)
EphB2	Decreasing gradient from bottom to top of crypt	(Batlle et al. 2002)
Math-1	Goblet + enteroendocrine + Paneth precursors	(Yang et al. 2001)
Hes-1	Proliferative cells (specific precursors?)	(Jensen et al. 2000)
Ngn-3	Enteroendocrine precursors	(Jenny et al. 2002)
Differentiated		
P21 waf1/Cip1	Cell cycle arrested cells	(van de Wetering et al. 2002)
Ephrin-B1	Gradient from surface epithelium to crypt bottom	(Batlle et al. 2002)
IHH	Top third and surface epithelium in adult colon	(van den Brink et al. 2004)
Carbonic anhidrase II	Top third and surface epithelium in colon	(van de Wetering et al. 2002)
Phospho-smad 1/5/8	Differentiated cells in villus	(Haramis et al. 2004)
Villin	Microvilli-increasing gradient from crypt to villus	(West et al. 1988)
FabpI/FabpL	Enterocytes	(van de Wetering et al. 2002)
Alkaline phosphatase	Enterocytes-brush border	(Reul et al. 1992)
Sucrose isomaltase	Enterocytes-brush border	(Reul et al. 1992)
Math-1	Mature goblet, enteroendocrine and Paneth cells	(Pinto et al. 2003)
Muc2	Goblet cells	(Gambus et al. 1993)
NeuroD/Beta	Enteroendocrine cells	(Naya et al. 1997)
Synaptophysin	Enteroendocrine cells	(Pinto et al. 2003)
Secretin	Enteroendocrine cells	(Roth & Gordon 1990)
Serotonin	Enteroendocrine cells	(Roth & Gordon 1990)
Lysozyme	Paneth cells	(Batlle et al. 2002)
Cryptdins	Paneth cells	(Selsted et al. 1992)
EphB3	Paneth cells	(Batlle et al. 2002)

(*) Referenced works contain details on expression patterns in the intestinal epithelium as well as on reagents and protocols to detect each marker on future sections.

Table 1

Additional genes affecting cell renewal in the intestine.

Gene	Function	Knockout phenotype	Reference
Fkh6	Forkhead homolog 6 Transcription factor	Expanded crypt compartment Hyperproliferative crypts Increased number of goblet cells Retarded formation and growth of nascent villi in late fetal period	[49]
Nkx2-3	NK 2 homeobox transcription factor	Expanded crypt compartment Hyperproliferative crypts Retarded formation and growth of nascent villi in late fetal period	[50]
Ihh	Indian Hedgehog Cell signalling molecule	Early postnatal lethality Reduced proliferation in the intervillar regions Reduced differentiation of endocrine cells	[51]
E2F4	Cell cycle regulator	Reduced or absent intervillar regions in late fetal period Reduced crypt compartment Hypoproliferative crypts Reduced number and smaller villi	[52]
Integrinβ4	Extracellular matrix membrane receptor	Early postnatal lethality Reduced proliferation in the intervillar regions Reduced number and smaller villi	[53]

A gastrointestinalis „stem cell niche”

- Musashi1 (RNS-kötő fehérje) és Hes-1 (lásd: Notch) koexpressziója a feltételezett stem sejtekben (Hes-1 egyedül expresszálódik a migráló progenitorokban)
- **Cdx-1** és **Cdx-2** (homeobox transzkripciós faktorok): Tcf-4 kontrollja alatt (lásd Wnt); proliferáció gátlása, differenciáció
- **Fox1** (forkhead box transzkripciós faktor): gastrointestinalis mezenchymára jellemző ⇨ HSPG-termelés ⇨ Wnt-Frizzled kötés erősödése ⇨ epitélium proliferációjának indirekt növekedése
- **Dickkopf** (Wnt receptorokhoz köt): proliferációt csökkenti
- TGFβ (BMP)-Smad-útvonal: magas **BMP4** expresszió a bolyhok közötti mezenchymában (de nem proliferatív régióban): a proliferáció gátlása, a Wnt-rendszer antagonizálásával (PTEN ⇨ PI3K ⇨ Akt gátlása, és így β-catenin gátlása)
-Ihh (indian hedgehog) -/- állatokban csökken a bélbolyhok száma (de nem a proliferáció csökkenése miatt)

A lieberkühn kriptát
• Intestinalis SubEpithelialis MyoFibroblastok (**ISEMF**) /SMA$^+$, desmin$^-$/ és
• Cajal féle sejtek (ICC) /SMA$^+$, desmin$^+$, c-kit$^+$, CD45$^+$/ veszik körül.

Wnt szignalizáció szerepe a bélhám őssejtjeinek szabályozásában

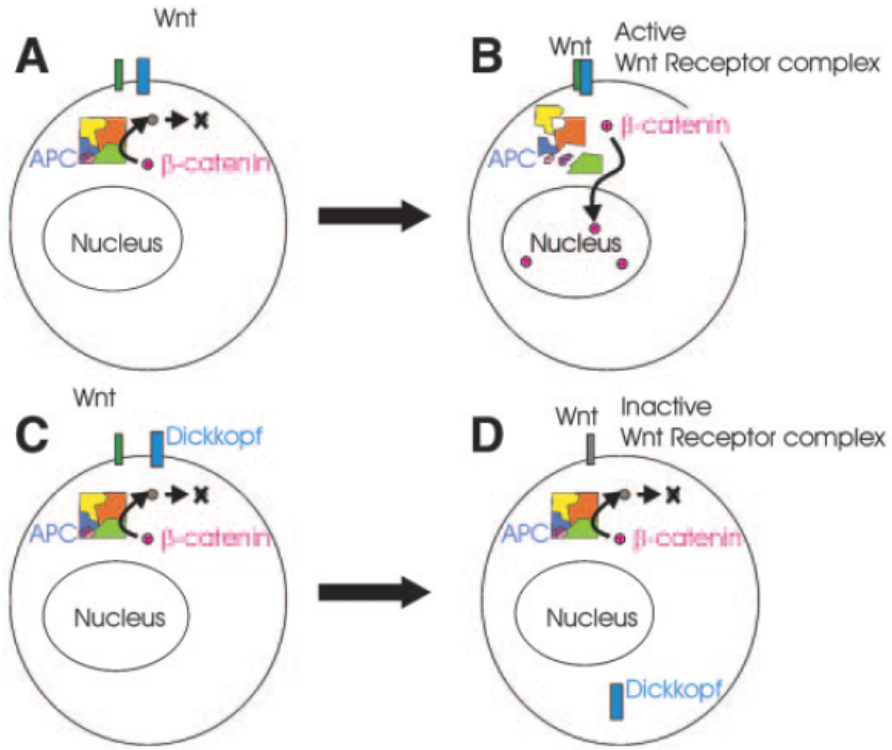

Fig. 2. Simplified Wnt signaling. *A*: in the absence of Wnt, an adenomatous polyposis coli (APC)-dependent protein complex inactivates β-catenin, targeting it for degradation (curved arrow). *B*: when Wnt binds its receptor complex, the APC-dependent protein complex is inactivated leading to an accumulation of active β-catenin in the nucleus, altering gene expression. Note that inactivating mutations in various components of the APC-dependent protein complex, including APC, can lead to a similar accumulation of active β-catenin in the nucleus, mimicking constitutive Wnt signaling. Wnt signaling can be suppressed by extracellular Dickkopf, which binds to a component of the Wnt receptor complex (*C*), inducing its internalization (*D*).

Canonical Wnt signals are essential for homeostasis of the intestinal epithelium

Daniel Pinto, Alex Gregorieff, Harry Begthel, and Hans Clevers[1]

GENES & DEVELOPMENT 17:1709–1713 © 2003

módszer: villin promóterrel kifejeztetett Dkk1

Essential requirement for Wnt signaling in proliferation of adult small intestine and colon revealed by adenoviral expression of Dickkopf-1

Frank Kuhnert*, Corrine R. Davis†, Hsiao-Ting Wang*, Pauline Chu†, Mark Lee*, Jenny Yuan*, Roel Nusse‡, and Calvin J. Kuo*§

266–271 | PNAS | January 6, 2004 | vol. 101 | no. 1

módszer: Dkk-t expresszáló adenovírus fertőzés

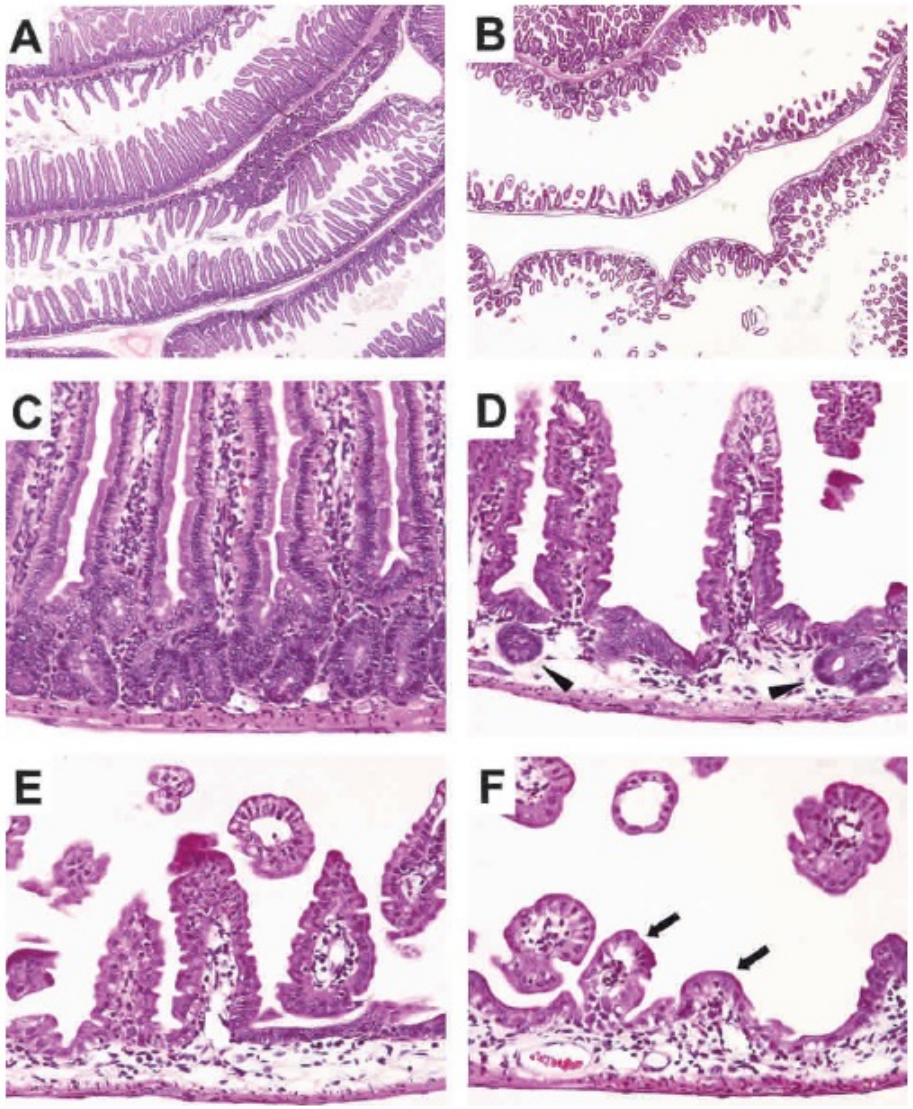

Figure 1. Dkk1 ectopic expression deleteriously affects crypt–villus organization. Representative sections of the small intestine from wild-type (*A,C*) and transgenic (*B,D–F*) adult animals stained with hematoxylin/eosin. The number and the size of crypts and villi are drastically reduced in the transgenic mucosa to rare residual crypt-like structures (arrowheads in *D*) or few residual villi (arrows in *F*).

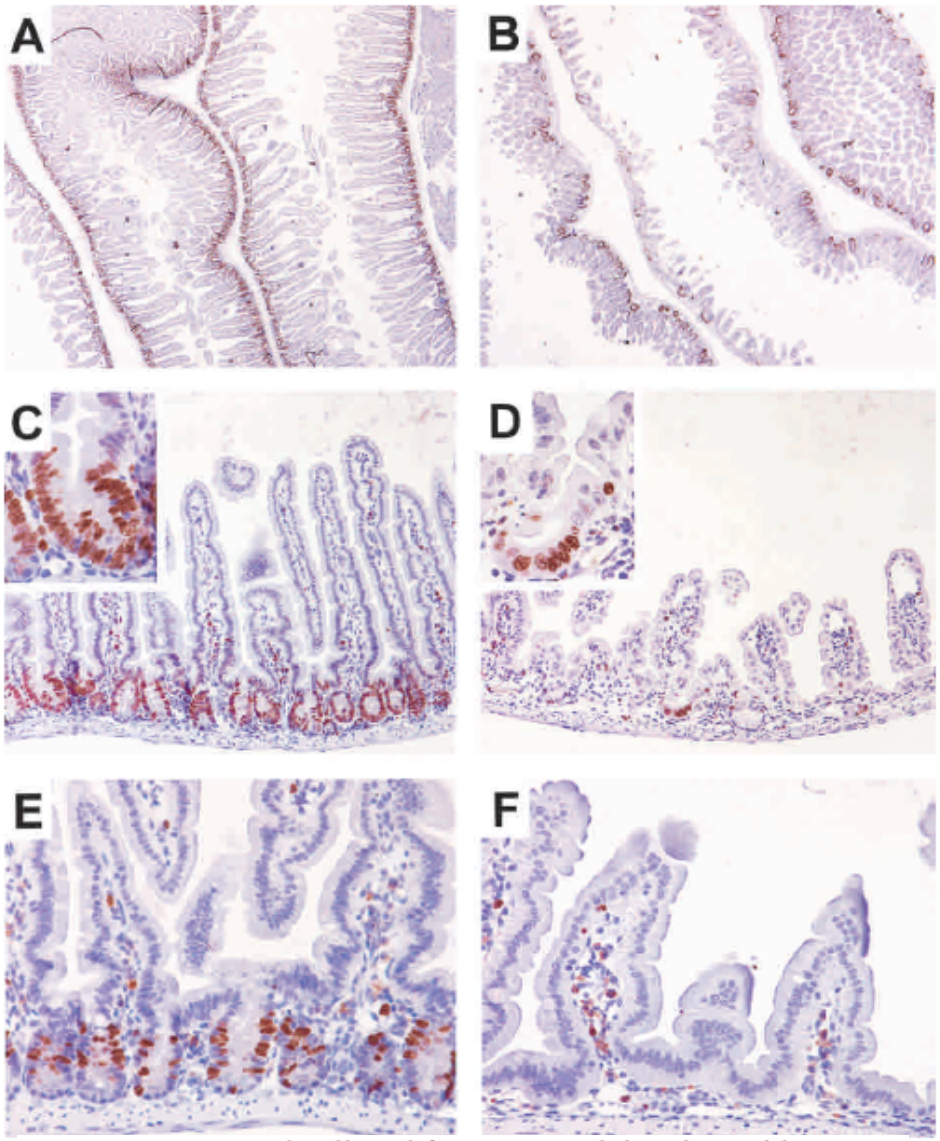

Figure 2. Intestinal cell proliferation is inhibited in Dkk1 transgenic mice. Immunohistochemical analysis of small intestine sections from wild-type (*A,C*) or transgenic (*B,D*) adult mice stained with an antibody against proliferating cell antigen Ki-67, and wild-type (*E*) or transgenic (*F*) adult mice labeled with BrdU and stained with an anti-BrdU antibody. Note that proliferative cells are abun-

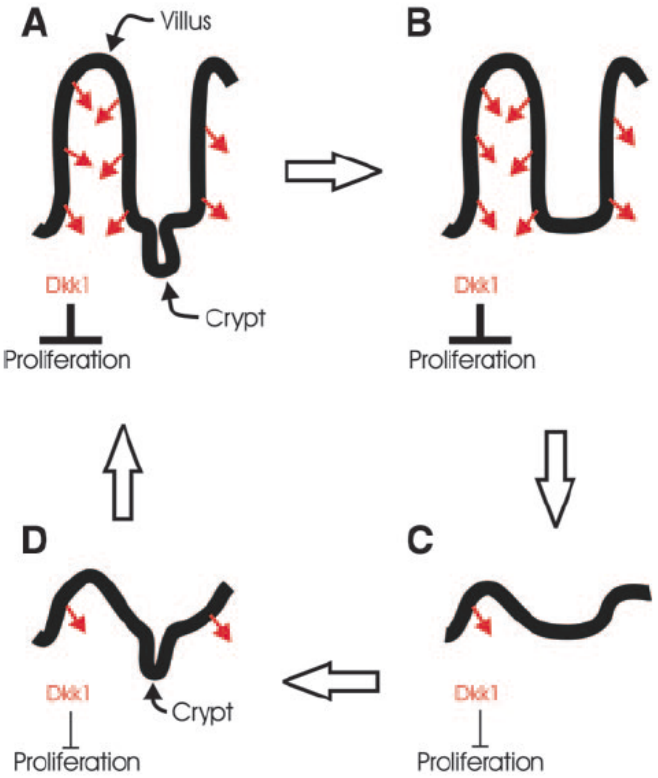

A Dkk1 túltermeltetése miatt összeesnek a bélbolyhok.

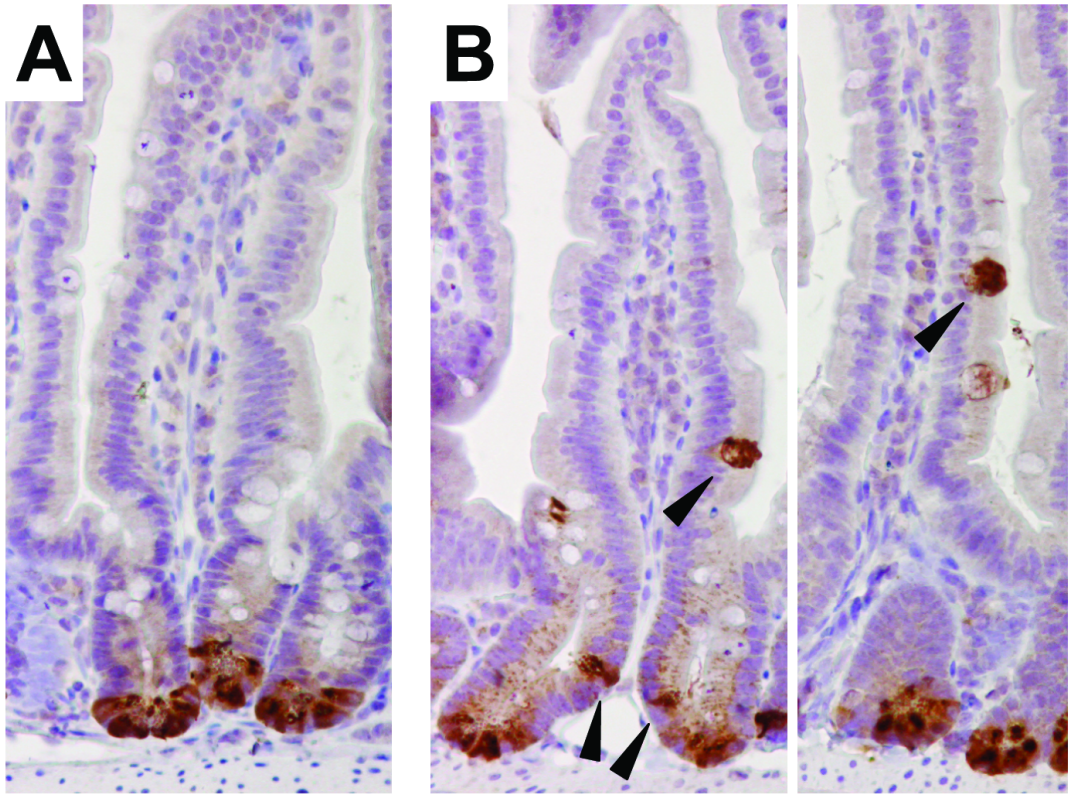

Dickkopf1 overexpresszió hatására a Paneth sejtek homing-ja elromlik

Mispositioning of Paneth cells in the small intestine of Dkk1 transgenic mice. Immunohistochemical analysis of small intestine sections from wild-type (*A*) or transgenic (*B*) adult mice stained with an antibody against lysozyme (Paneth cell marker), showing Paneth cells aberrantly allocated in crypts and villi of transgenic specimens (arrowheads).

Mi a helyzet a Wnt útvonal túlaktivációja esetén?

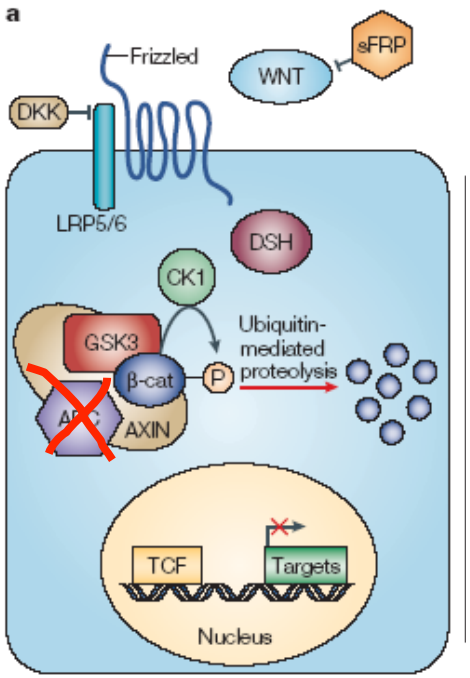

Wnt-β-catenin rendszer:
(human colorectalis tumorok 85%-ában mutáns az APC – v.ö.: adenomatous polyposis)

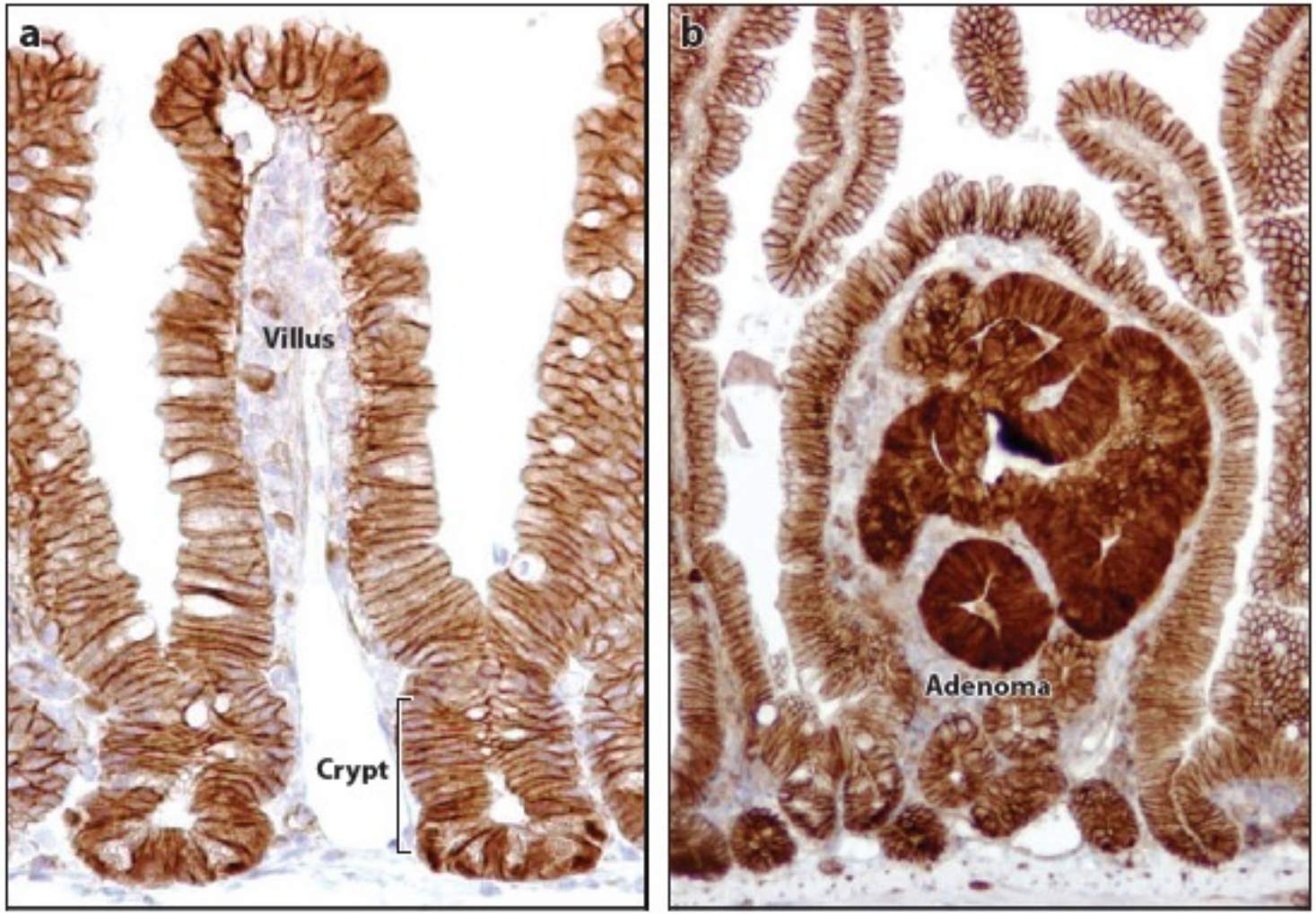

Figure 3

Active Wnt signaling in the intestine. Nuclear β-catenin is a hallmark for active Wnt signaling. (*a*) β-Catenin staining in normal wild-type intestinal epithelium. On the villus only the membranes stain positive, and at the bottom of the crypts postmitotic Paneth cells also show nuclear β-catenin staining. (*b*) Early adenoma tissue surrounded by wild-type crypt and villus epithelium in an Apc^{min} mouse shows elevated β-catenin levels in the adenoma cells, indicating hyperactive Wnt signaling.

Wnt szignalizáció

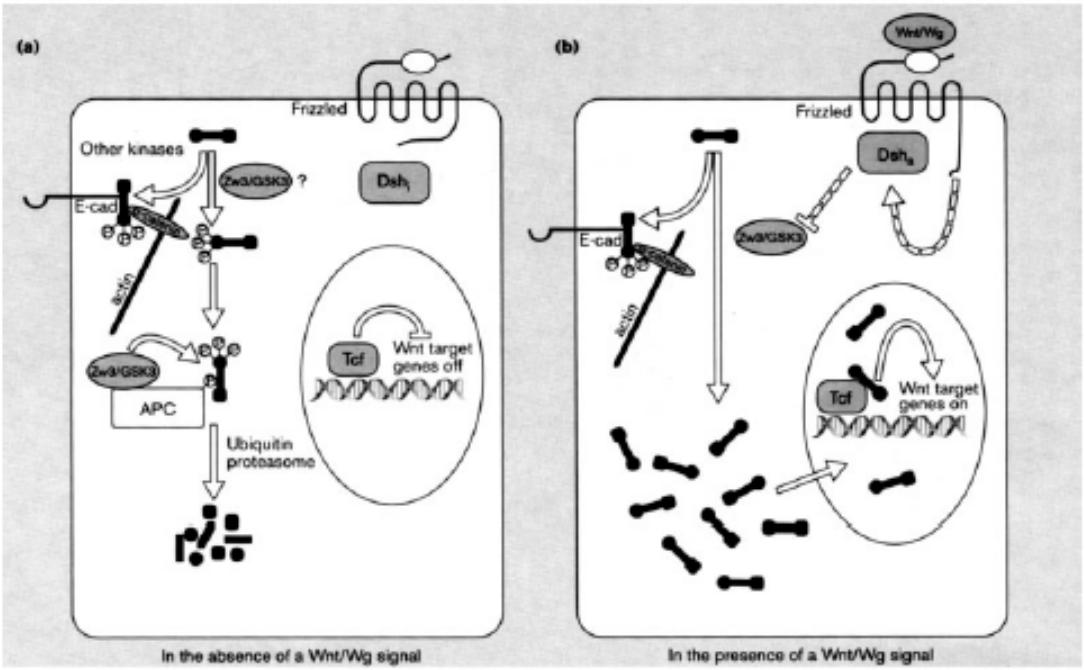

Figure 7. The Wnt signalling pathway. In the absence of Wnt signalling, Dishevelled is inactive (Dsh_I) and *Drosophila* Zeste-white 3 or its mammalian homologue glycogen synthase kinase 3 (Zw3/GSK3) is active. β-Catenin (black dumb-bell), via association with the APC-Zw3/GSK3 complex, undergoes phosphorylation and degradation by the ubiquitin–proteasome pathway. Meanwhile, TCF is bound to its DNA-binding site in the nucleus, where it represses the expression of genes such as Siamois in *Xenopus*. (b) In the presence of a Wnt signal, Dishevelled is activated (Dsh_A), leading to inactivation of Zw3/GSK3 by an unknown mechanism. β-Catenin fails to be phosphorylated and is no longer targeted into the ubiquitin–proteasome pathway. Instead, it accumulates in the cytoplasm and enters the nucleus by an unknown pathway where it interacts with TCF, to alleviate repression of the downstream genes and provide a transcriptional activation domain (from ref. 80, with permission)

1. proliferáció szabályozás
2. migráció szabályozás (EphB)
3. differenciáció szabályozása

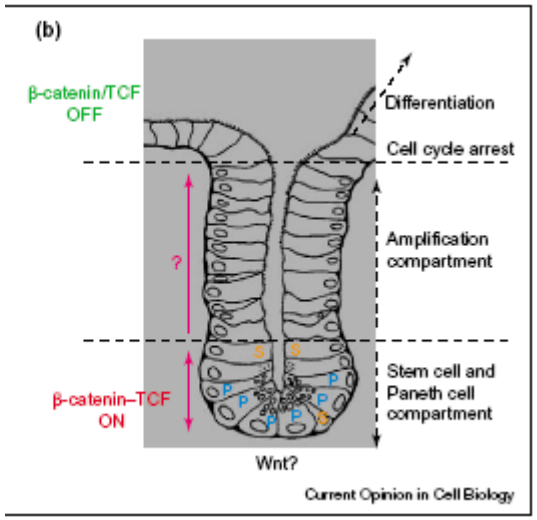

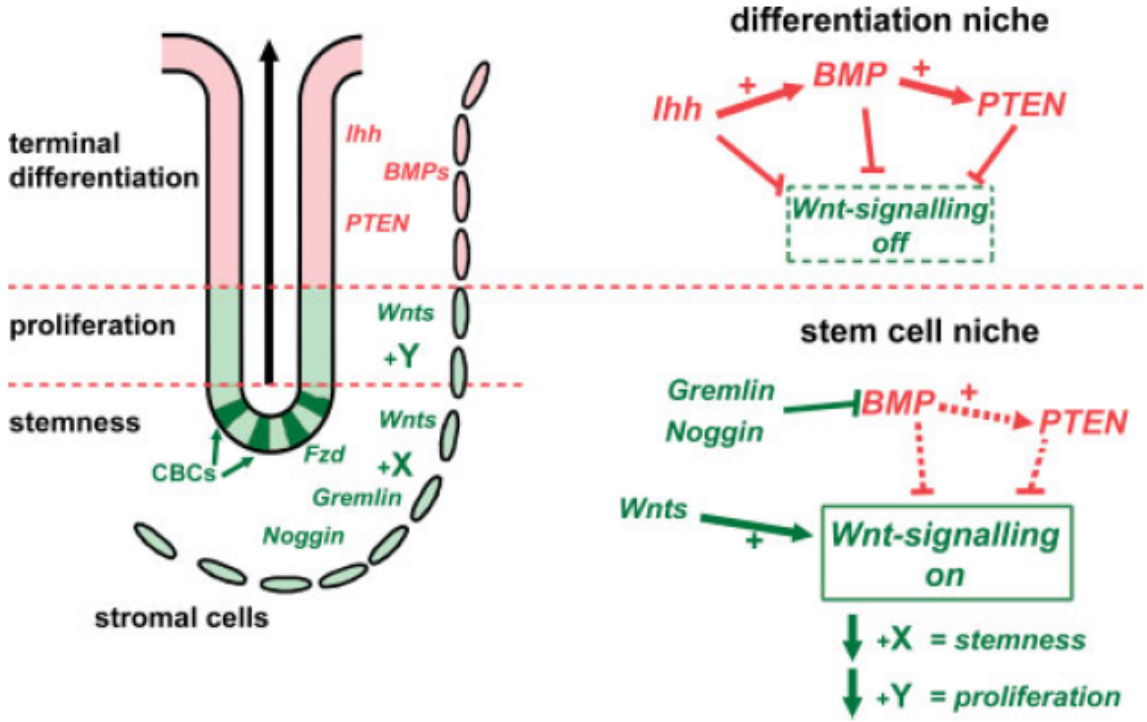

Figure 2. Putative intestinal stem cell niche. Scheme of the architecture and signalling in the mucosa of the large intestine (left). Red indicates differentiated cells and pathway components inducing differentiation. Green indicates stem cells (CBCs), transit-amplifying cells or signalling inducing it. A simplified view of the stem cell niche, which might turn out be much more complex (right): putative signalling crosstalks defining the stem cell niche and the differentiating cell niche. In the upper crypt regions, indian hedgehog (Ihh) triggers BMP expression in stromal cells, which then activates PTEN expression in epithelial cells. All three factors directly or indirectly inhibit Wnt signalling. In the stem cell niche, surrounding stromal cells secrete the BMP inhibitors Noggin and Gremlin, leading to a relief of repression of Wnt signalling. In addition, the stroma provides Wnt ligands to induce Wnt signalling through Fzd receptors in stem cells and transit-amplifying cells. Additional unknown signals specify Wnt signalling towards expression of stem cell-associated target genes (X) or proliferation-associated target genes (Y)

Gastrointestinalis epithelium

Az egyes fejlődési irányok szétválása: Notch/Delta

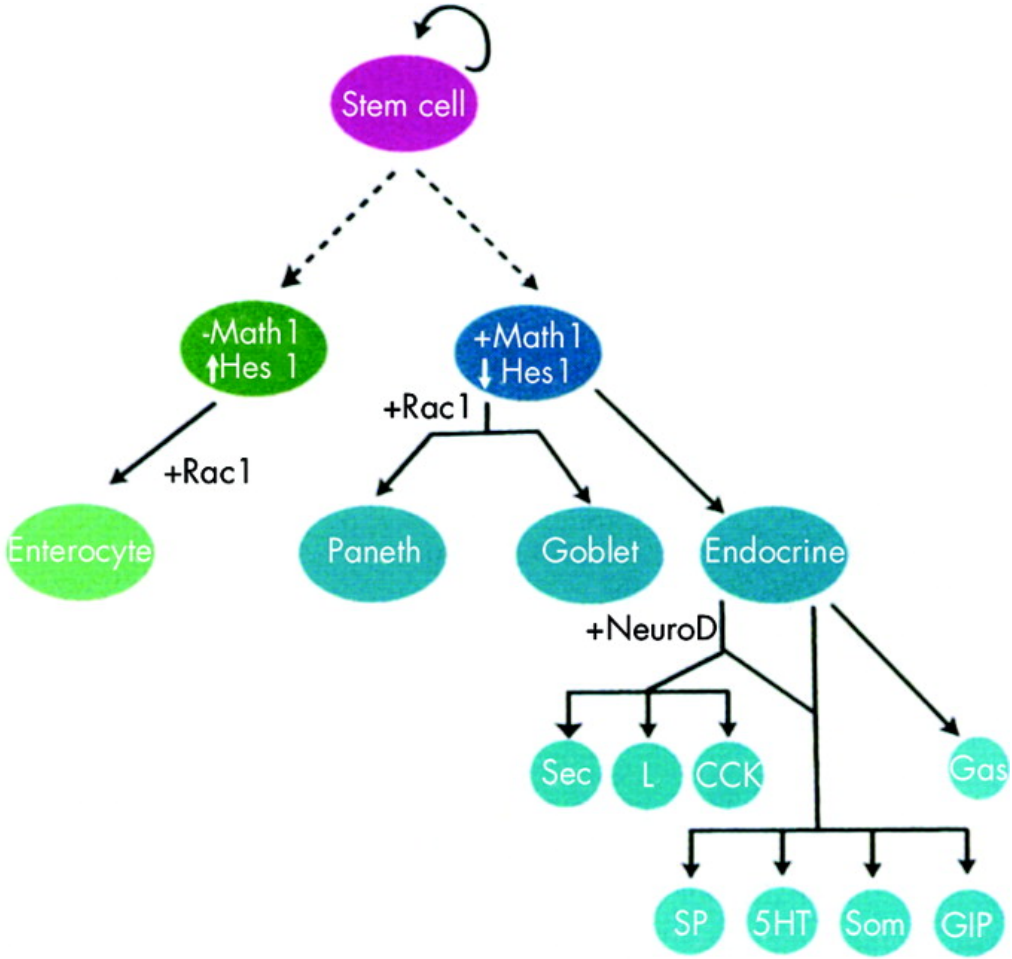

Goblet sejt (mucin

Enterociták (alkalikus foszf

A Notch/Δ rendszer a **Math1** („proszekretoros gén”) bHLH transzkripciós faktoron keresztül szabályozza az enterocita/szekret sejt fejlődési irányokat.

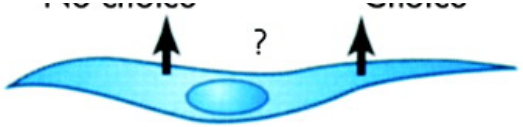

Prekurzorok (PCNA-festés)

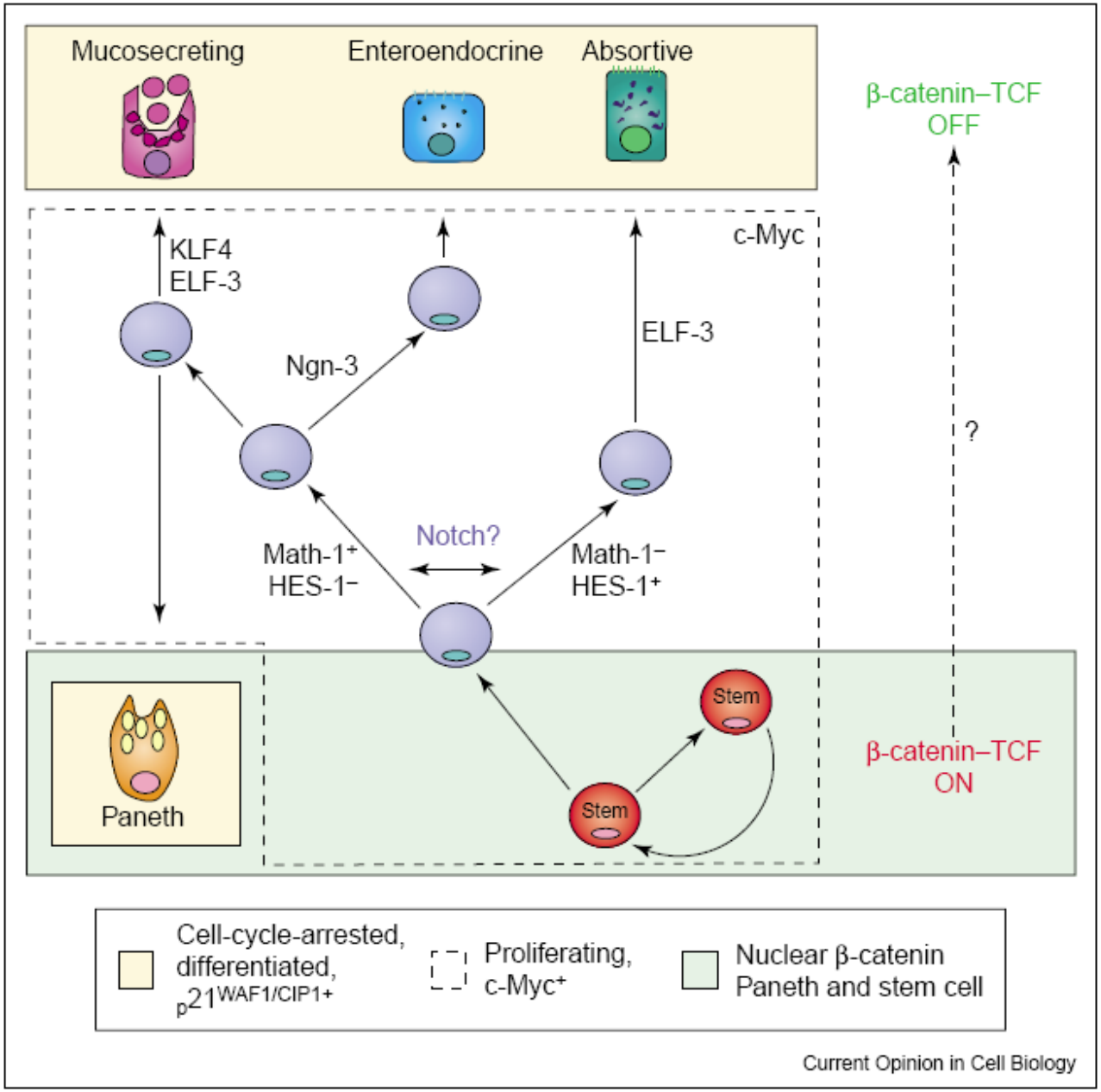

Sejtsors meghatározása

Notch: γ-secretase gátlása (Alzheimer gyógyszer) gastrointestinális problémákat okozott. (nagyon sok szekretoros sejt lett)
Hasonló fenotípust mutatott a Hes1$^{-/-}$ fenotípus is

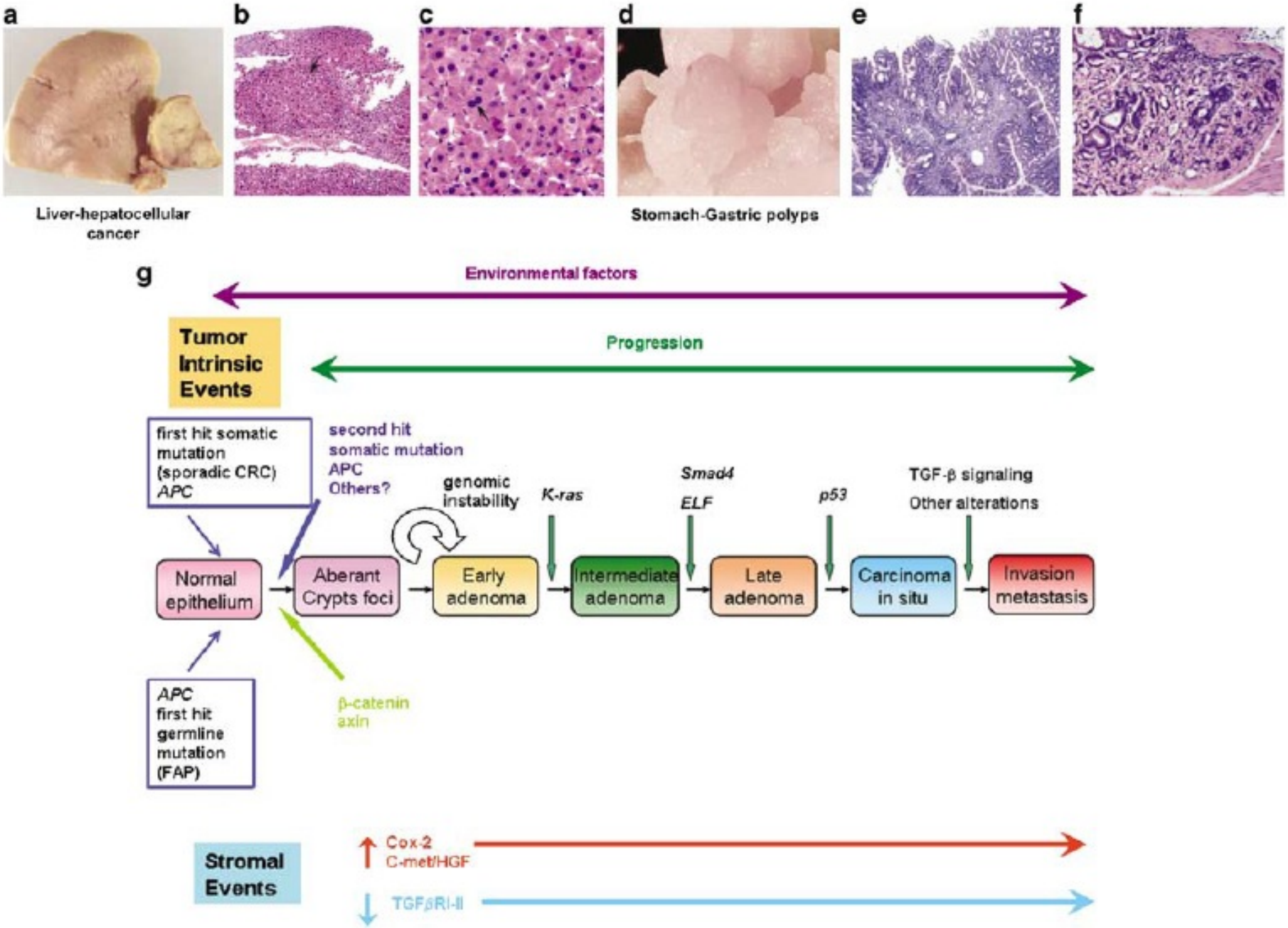

Figure 4 (a–c) Liver-hepatocellular cancer, (d–f) stomach-gastric polyps. (g) Schematic diagram to show APC inactive mutation and TGF-β signaling alteration during gastrointestinal tumor progression

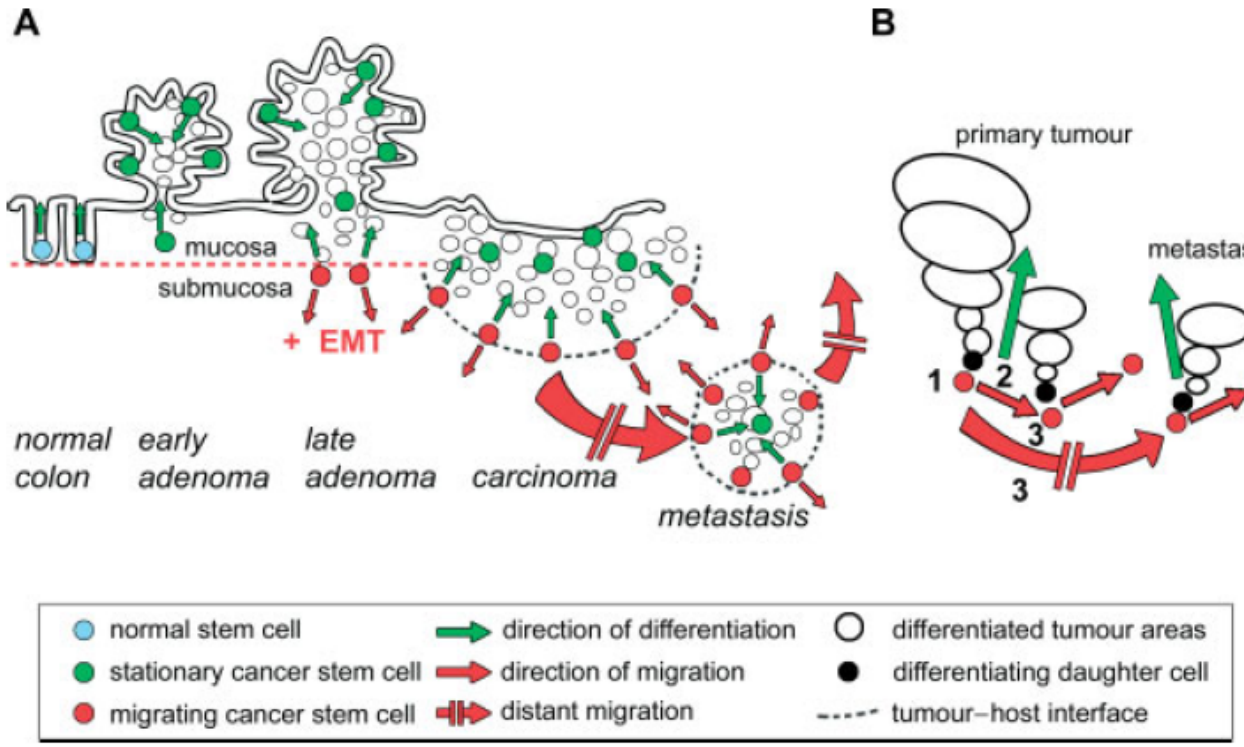

Figure 5. The migrating cancer stem cell (MCS cell) concept. (A) Normal stem cells (expressing nuclear β-catenin) are located at the crypt base of normal colon mucosa. Stationary cancer stem (SCS) cells are embedded in benign adenomas and might still be detectable in differentiated central areas of carcinomas and metastases. A crucial step towards malignancy is the induction of an epithelial–mesenchymal transition (EMT) in tumour cells, including SCS cells, which now become mobile, migrating cancer stem cells (MCS) cells. This step could be activated by aberrant environmental signals [in the example of colorectal cancer, after crossing the border of mucosa to submucosa (lamina muscularis mucosae) in late adenomas]. (B) Detailed view on MCS cells in carcinomas and metastases. MCS cells divide asymmetrically; one daughter cell starts proliferation and differentiation (1). The remaining MCS cell either migrates a short distance before new asymmetrical division, thereby adding mass to the primary tumour (2), or eventually starts long-range dissemination through the blood or lymphatic vessels and builds up a metastasis after subsequent asymmetrical divisions (3). Thus, the basic mechanisms are the same for primary carcinomas and metastases (adapted from [103])

A máj és a hasnyálmirigy fejlődése

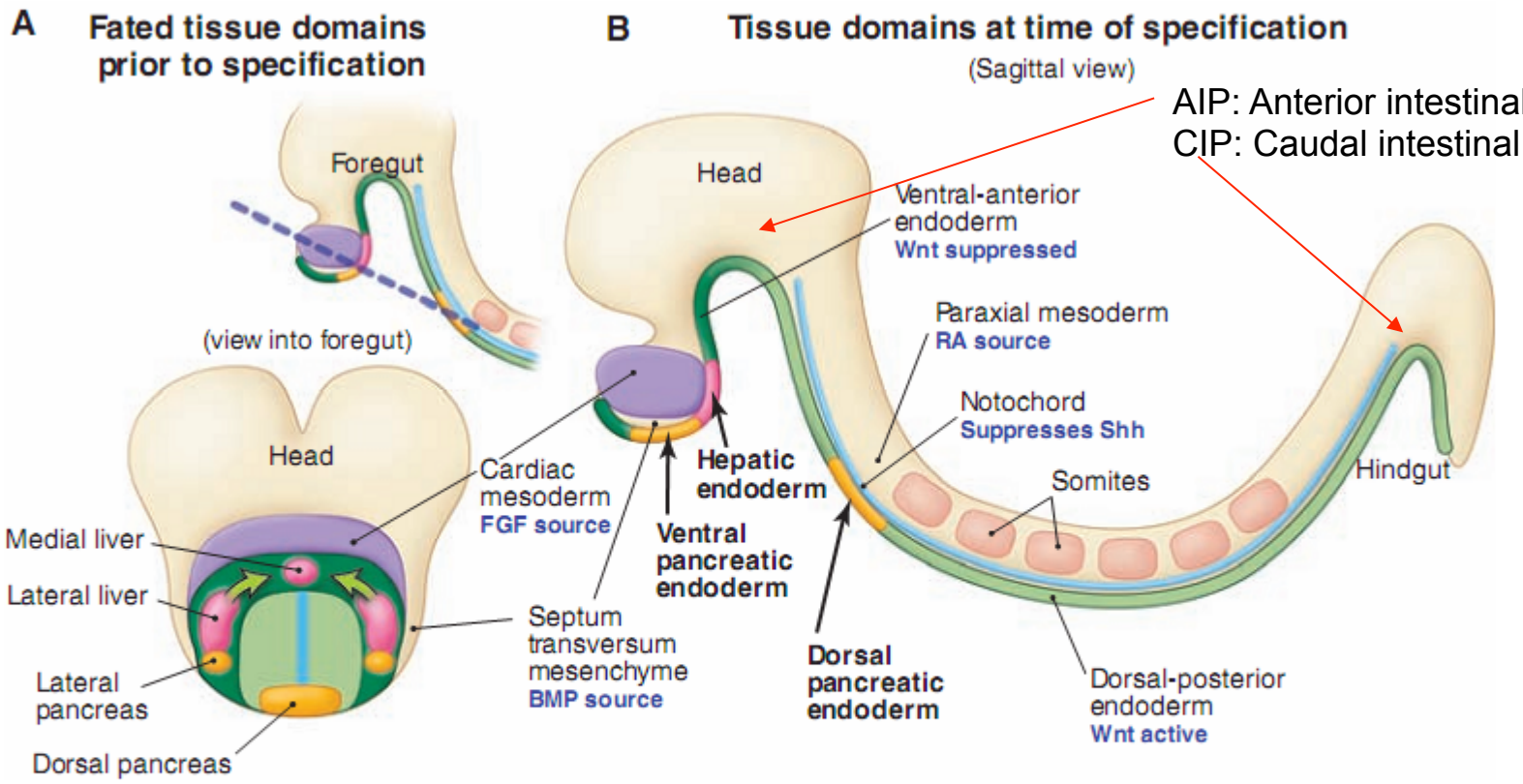

Fig. 1. Cell domains and signals for embryonic liver and pancreas specification. (**A**) Fate map of progenitor cell domains before tissue induction; view is into the foregut of an idealized mouse embryo at E8.25 (three- to four-somite stage). Green arrows indicate movement of lateral progenitor regions toward the ventral-medial region. (**B**) Sagittal view of a mouse embryo several hours later than in (A) showing the positions of the newly specified liver and pancreas tissue domains. Signals and cell sources that pattern the endoderm are shown. Dashed blue line indicates plane of view in (A).

A májbimbó fejlődésének állomásai egérben

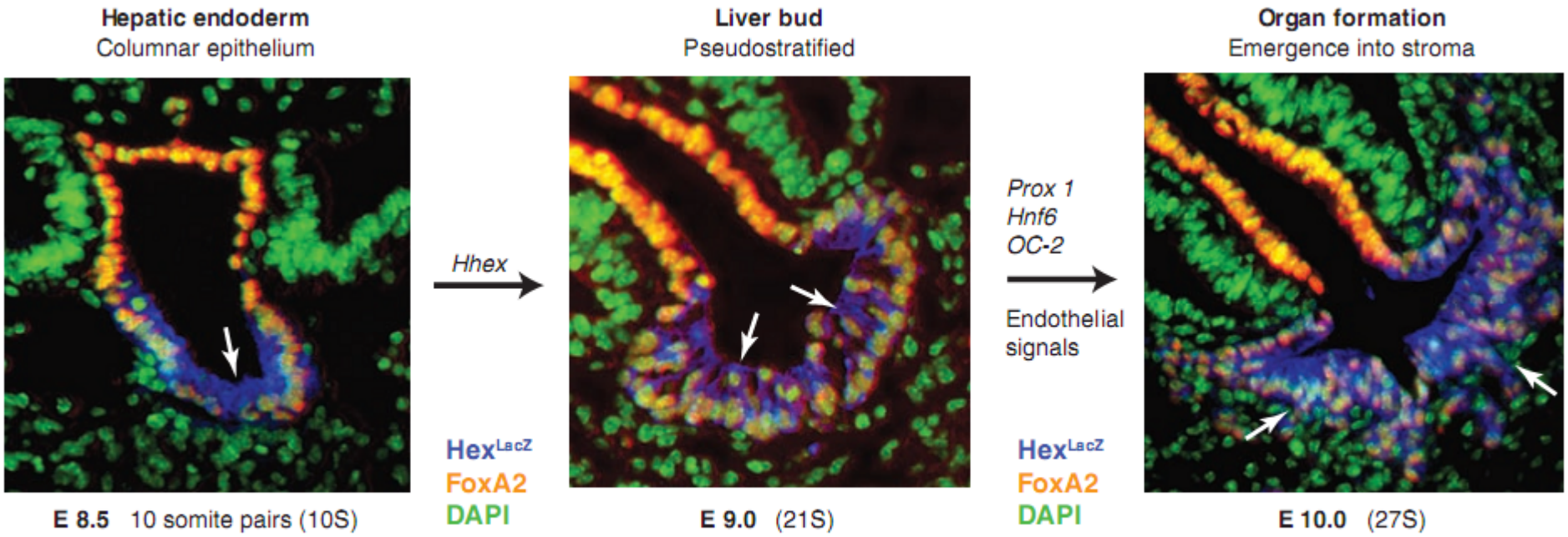

Fig. 2. Stages of liver bud organogenesis. Hepatoblasts are stained blue (Hex^{LacZ+}), cells with orange nuclei are gut endoderm ($FoxA2^{+}$), and all nuclei were stained green by 4′,6′-diamidino-2-phenylindole. White arrows point to the hepatic cells. Genes and signals that promote each transition are indicated. Similar morphogenetic stages occur during pancreas bud organogenesis. Images are adapted from (*36*). S, pair somite stage; E, embryonic day.

Hepatoblaszok
Bél endoderma sejtek
Sejtmagok

A máj és a hasnyálmirigy sejtjeinek leszármazási vonalai

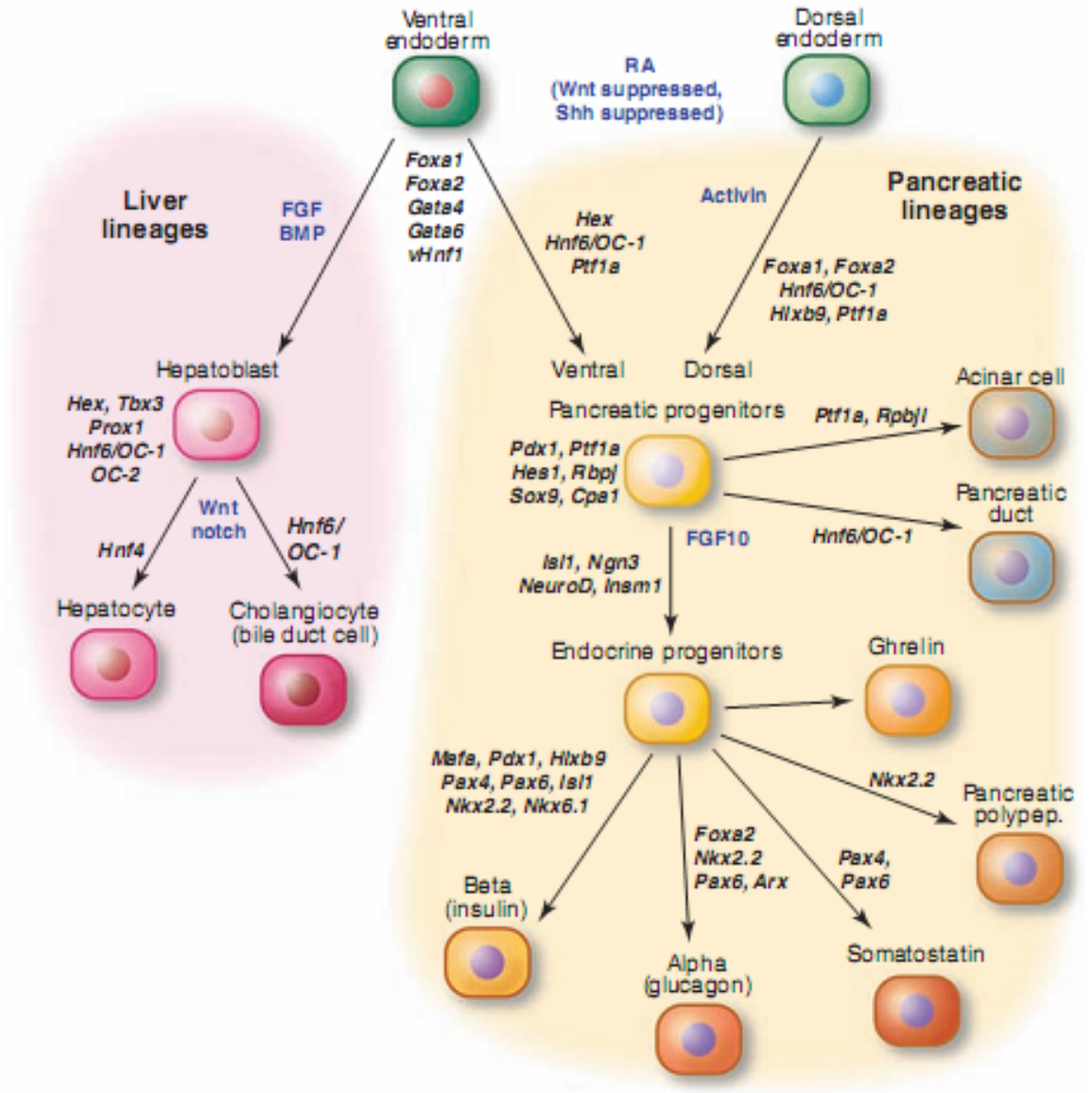

Fig. 3. Regulatory factors controlling cell type lineages within the liver and pancreas. Transcription factor genes are shown in bold; their functions have been reviewed in the text and elsewhere (*23*, *55*–*57*), except for *vHnf1* in hepatic development (*81*). *Pdx1* initially marks duodenum and caudal stomach progenitors (not shown) as well as the pancreatic domains (*28*).

Máj lebenyke szerkezete

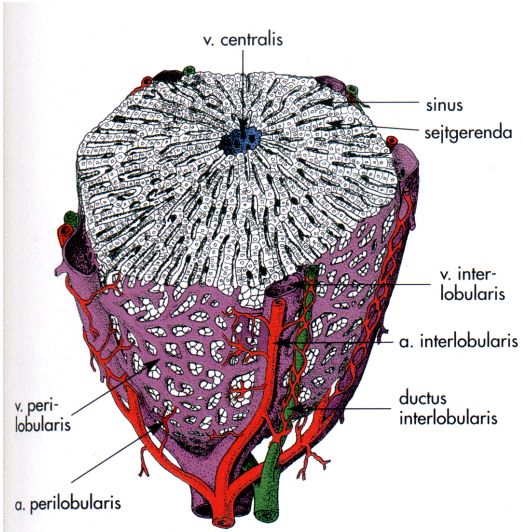

14-12. ábra. A lobulus hepatis térbeli ábrázolásban. A közel hatszögletű hasáb alakú májlebenyke közepén halad a v. centralis, míg az éleken az a., v. és ductus interlobularisokat (portális triász) találjuk (Krstic után).

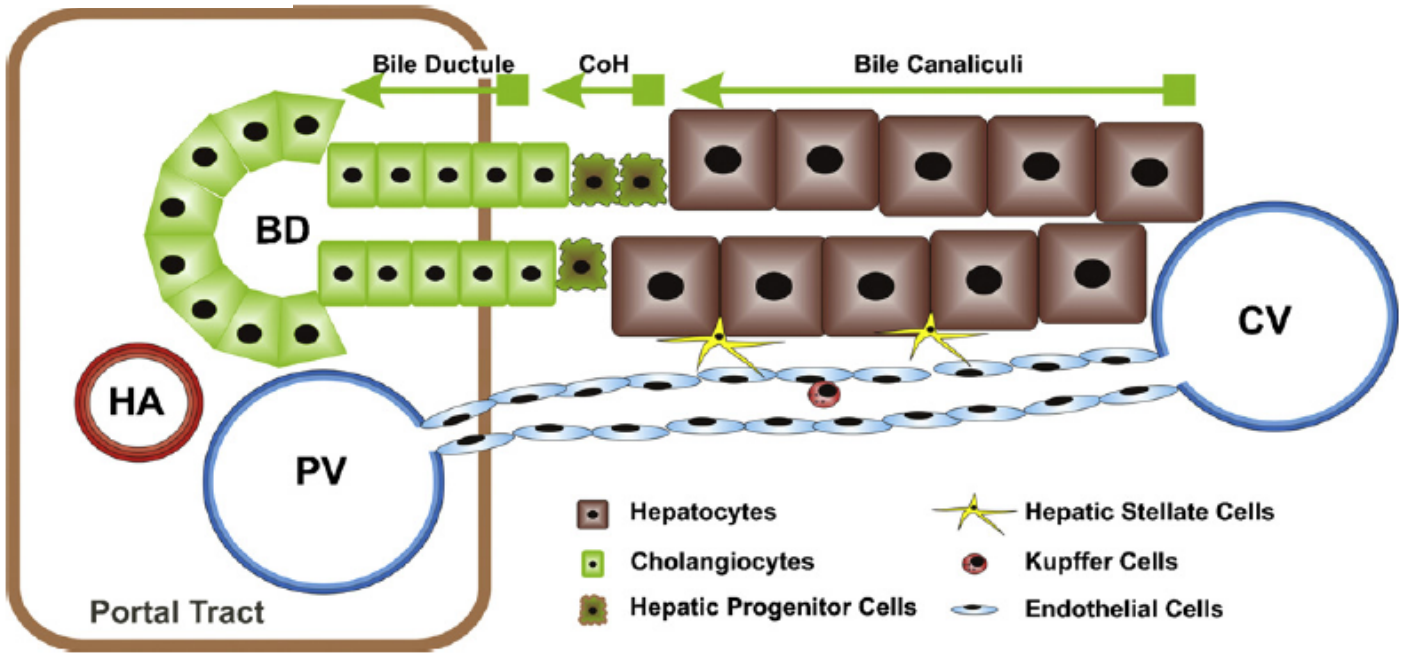

Fig. 1. Location of hepatic progenitor cells niche within the liver. Progenitor cells are located in the canals of Hering which represent the connection between bile canaliculi and bile duct systems.

2. Máj

- **LSPC** (Liver Stem/Progenitor Cell): egyelőre nincs in vivo bizonyíték arra, hogy valódi, önmegújításra képes őssejtek volnának a májban (avagy csak köztes sokszorozó).
- Az érett májsejtek (egy része?) azonban képes osztódni, hepatocyta/ cholangiocyta irányba in vivo (normál ill. sérülés esetén) és in vitro differenciálódni.
- Extrém regenerációs / transzdifferenciációs képesség

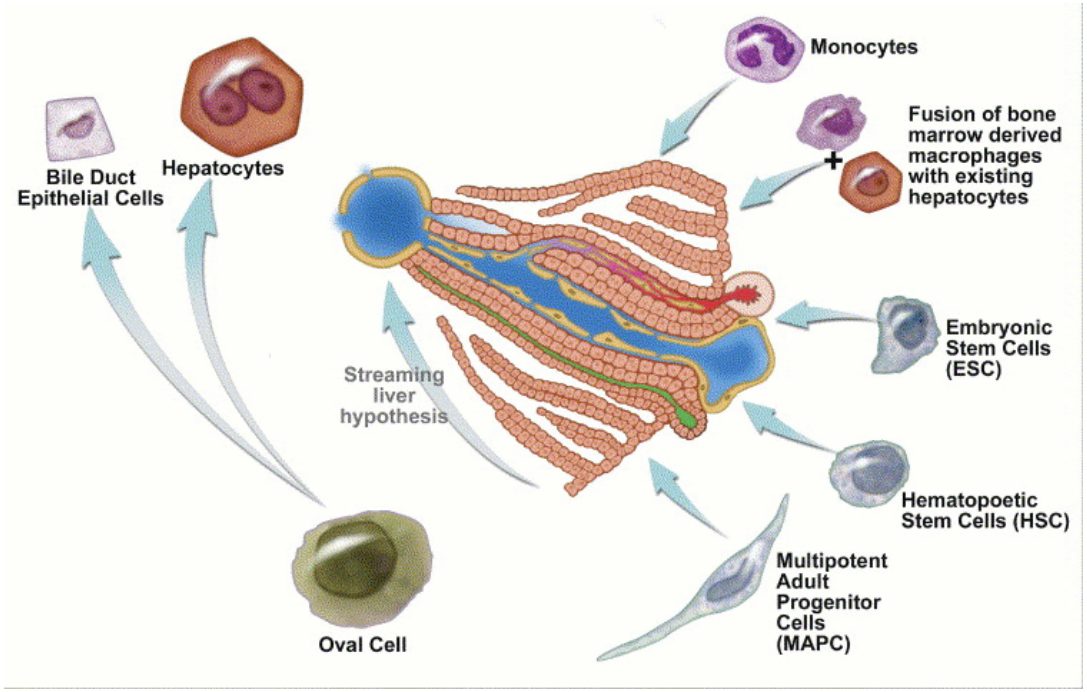

2. Máj

A máj „stem cell niche”

- a sejtek folyamatos, gyors turnovere: precízen szabályozott (és plasztikus) „stem cell niche”-re van szükség

- helyszíne: feltehetőleg a Hering-féle csatornák
- stem cell marker: nem ismert
- funkcionálisan azonosíthatók (BrdU, ^{3}H-timidin)

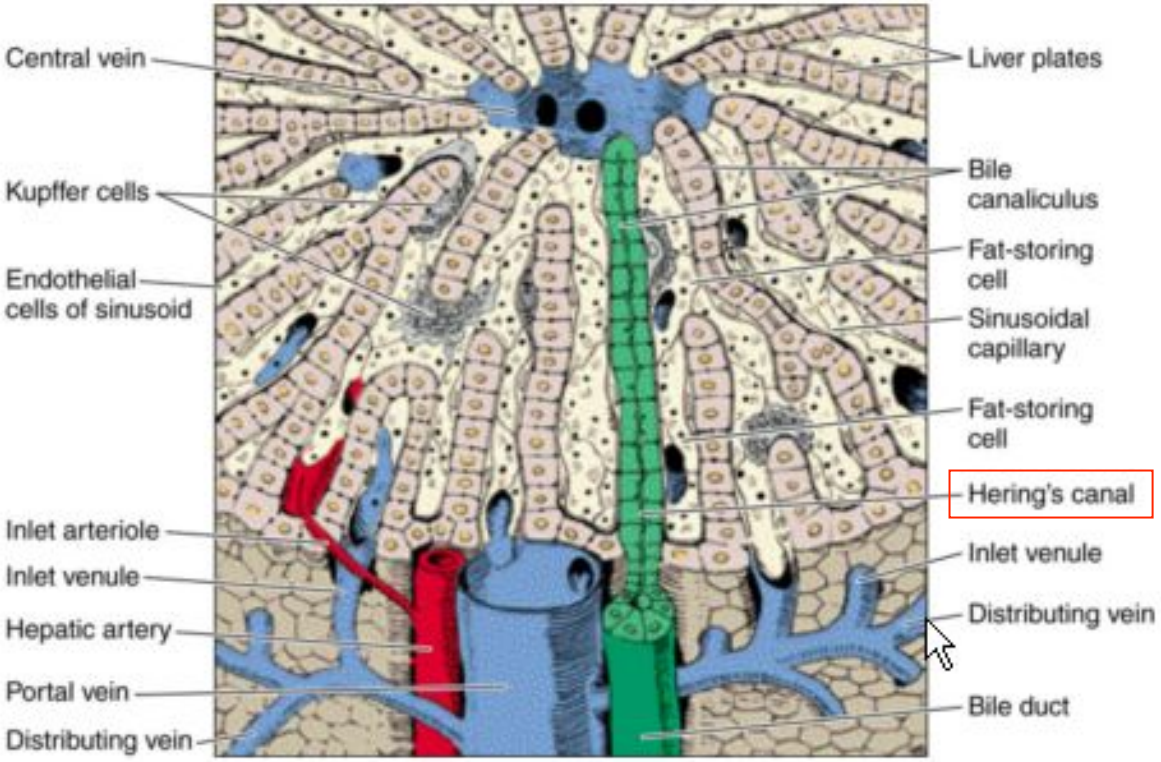

2. Máj

A máj „stem cell niche”

- sejt-sejt kapcsolatok: érdekes módon Notch/Delta rendszert még nem írták le a májban (kivétel: epecsatorna-epitél, ill. embrionális vérképzés)
- sejt-mátrix kapcsolatok: még csak leíró jellegű adatok a Hering-csatornával kapcsolatban, semmi funkcióra vonatkozó elképzelés
- Innerváció lehetséges szerepe; NGF, BDNF, neurotrophin-3, -4

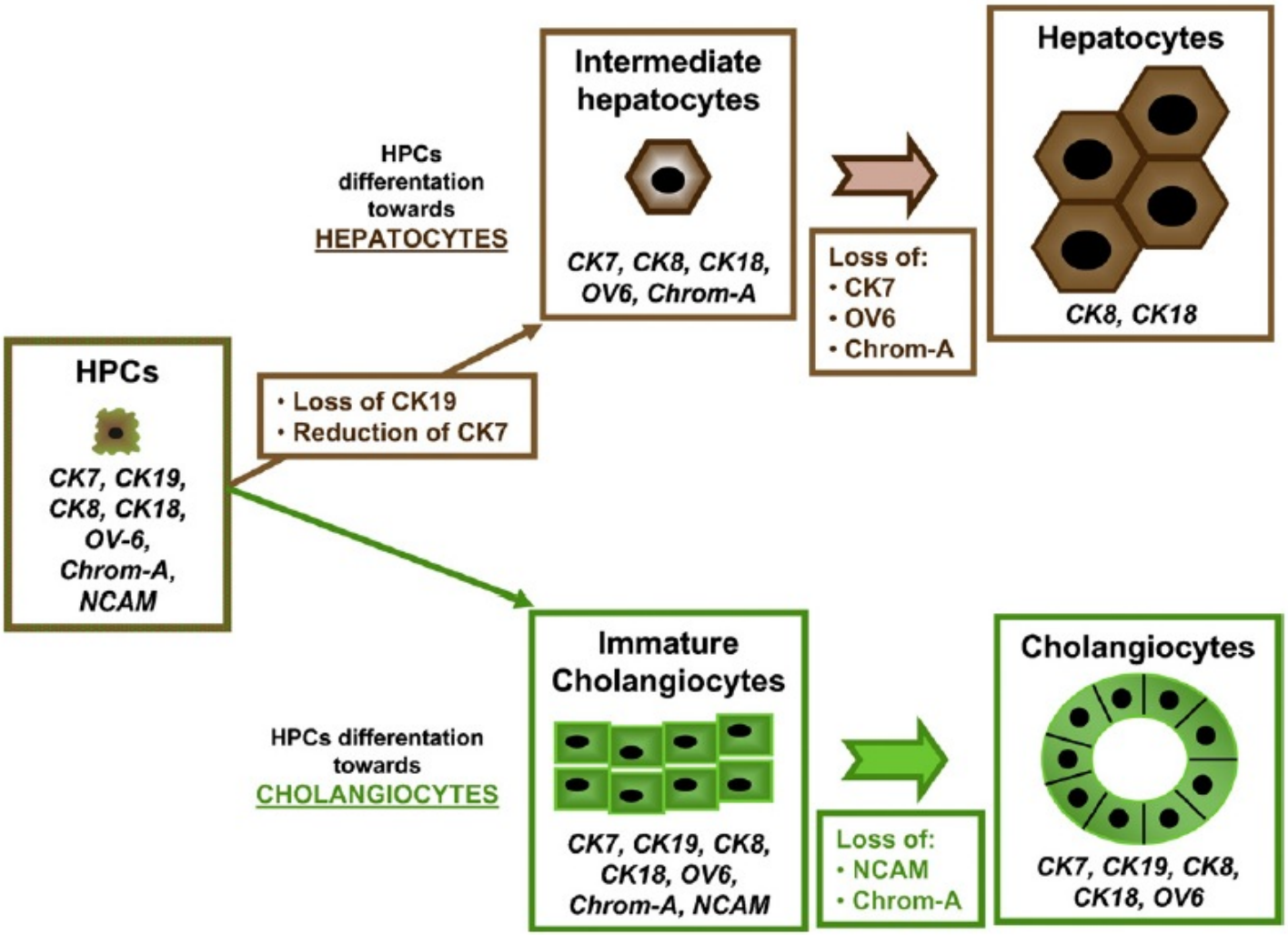

Fig. 2. Differentiation of hepatic progenitor cells towards mature hepatocytes or cholangiocytes. This process is characterized by the appearance of trans-amplifying populations represented by intermediate hepatocytes and reactive ductules.

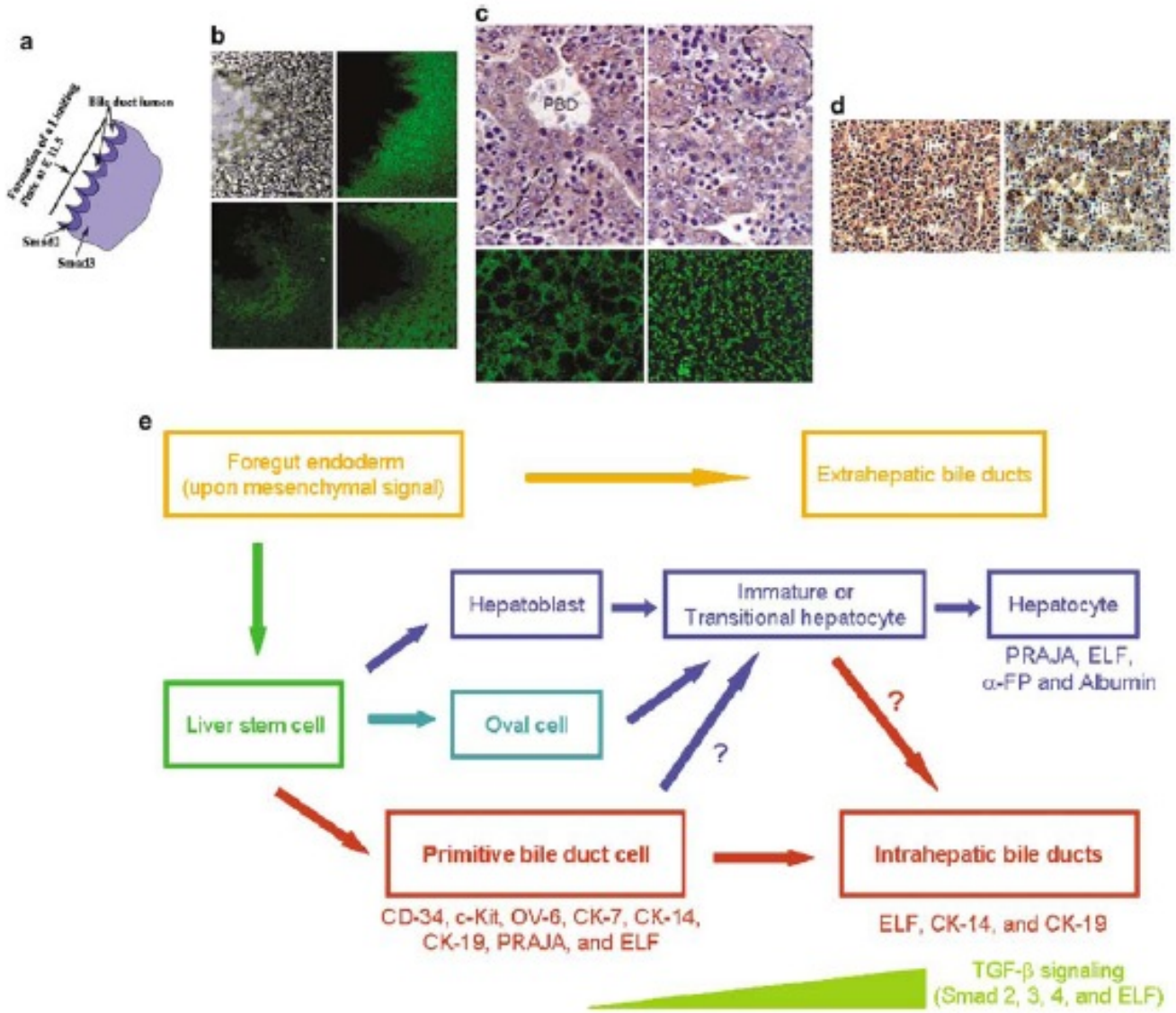

Figure 2 (a, b) Immunofloresecence labeling of Smad3 and Smad2 antibody show limiting plate with bile duct formation in *Smad2*$^{+/-}$/*Smad3*$^{+/-}$ liver explants by the addition of TGF-β. (a) Transmission picture of *Smad2*$^{+/-}$/*Smad3*$^{+/-}$ liver explants showing limiting plates with bile duct formation. (b) *Smad2*$^{+/-}$/*Smad3*$^{+/-}$ liver explants stained with Smad3 antibody, arrows point to limiting plates. (c, d) Loss of hepatocyte architecture and absence of primitive bile ducts (PBD) in *Smad2*$^{+/-}$/*Smad3*$^{+/-}$ mutant livers at E 11.5. (e) As the TGF-β signaling increases, bililary and epithelial cell differentiation occurs. Hierarchy of events as liver development occurs (Alpini *et al.*, 2004)

3. Hasnyálmirigy

- E8,5: **Pdx1** és **Hlxb9** (homeobox transzkripciós faktorok)
- E9,5-E11,5 között **Pdx1** expresszió ⇨ ductalis sejtek ⇨ endokrin/acinus sejtek
- **Notch^{high}**: ductalis, **Notch^{low}**: endokrin/acinus vonal
- a további fejlődés egyelőre kevéssé világos; **EGF**, **FGF10** szerepe
- E12,5: citokeratinok, mint korai ductalis markerek megjelenése

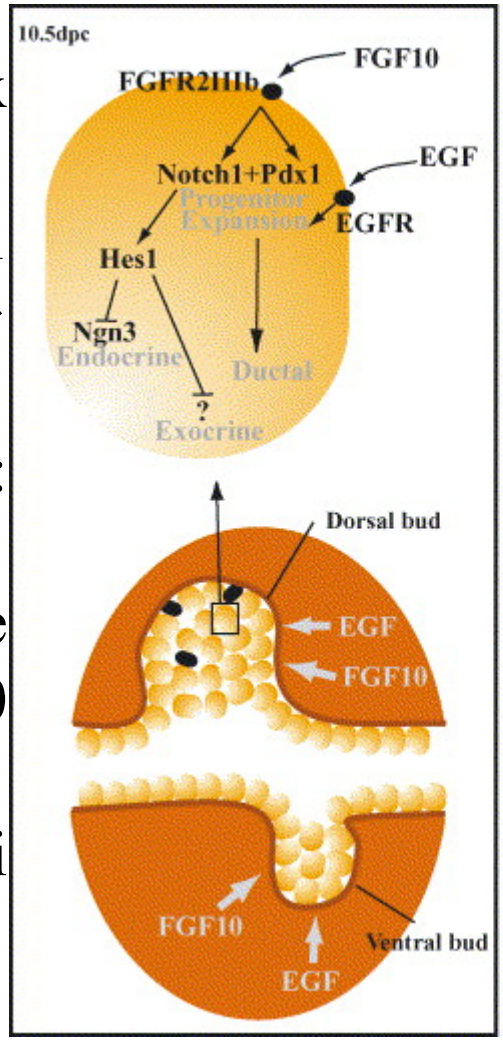

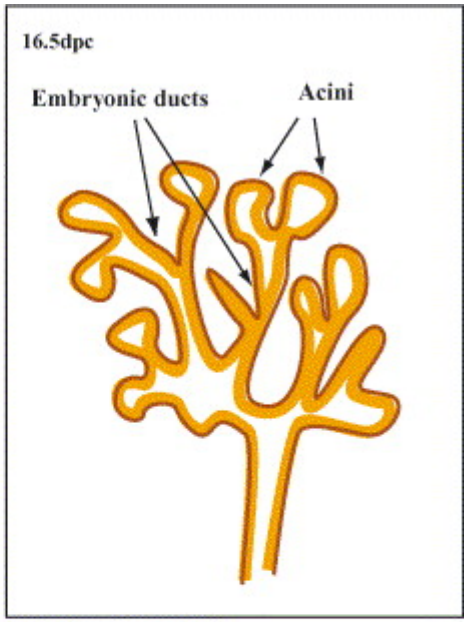

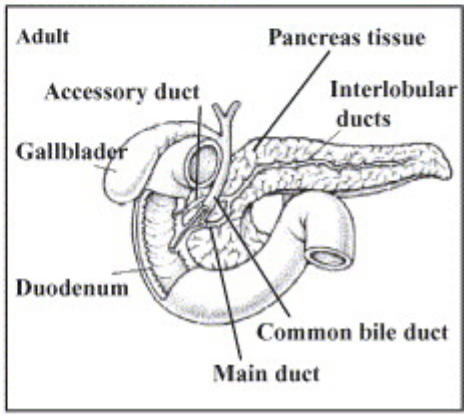

3. Hasnyálmirigy (β-sejtek)

Egy gyakorlati kérdés: csináljunk β-sejtet!

Létezik-e egyáltalán β-őssejt?

Raewyn M Seaberg, …, Derek van der Kooy *Nature Biotechnology* 22, 1115 – 1124 (2004)
Clonal identification of multipotent precursors from adult mouse pancreas that generate neural and pancreatic lineages

Yuval Dor, et al., *Nature* 429, 41-46 (6 May 2004)
Adult pancreatic β-cells are formed by self-duplication rather than stem-cell differentiation

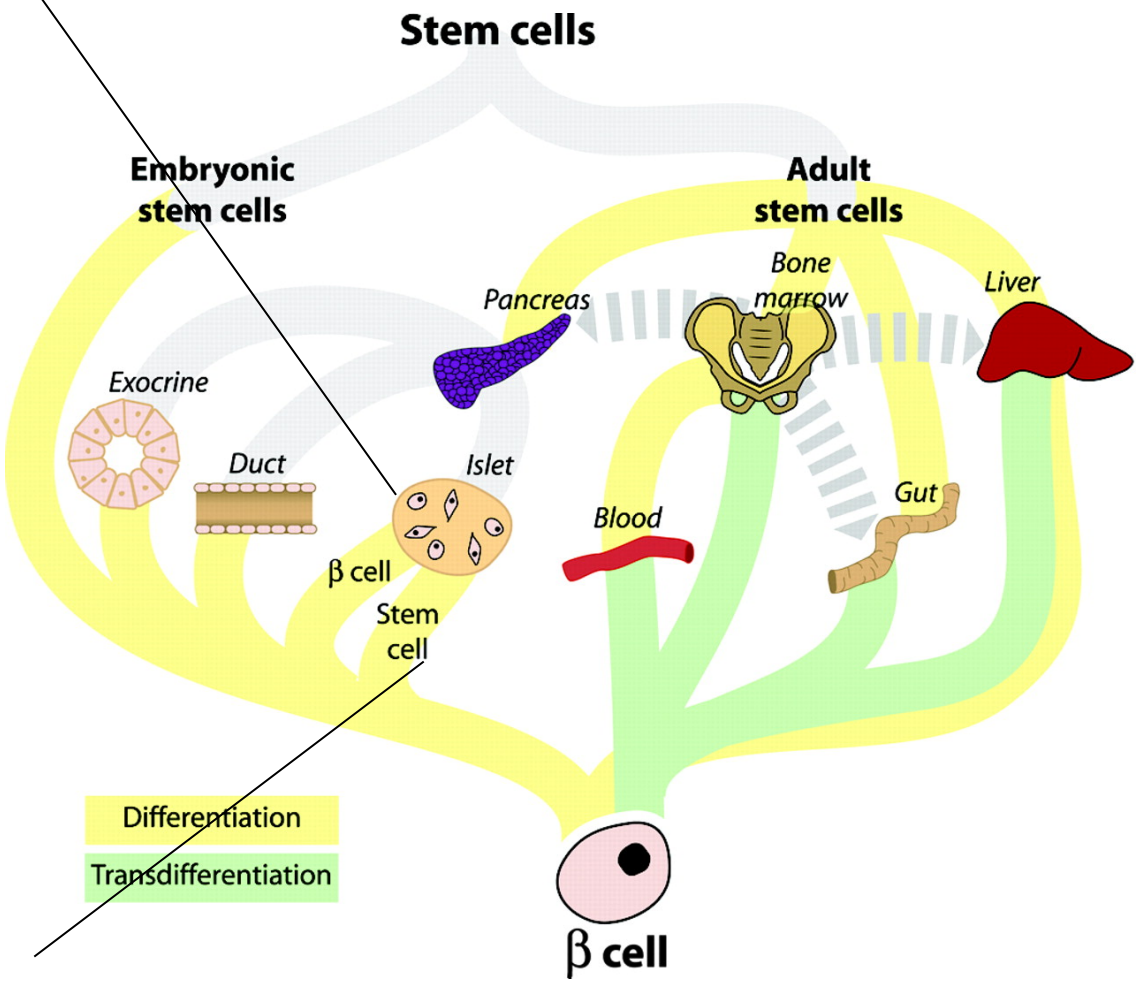

Hasnyálmirigy ős/progenitor sejt jelöltek:

1. Vezeték sejtek
2. Exocrine sejtek
3. Nestin pozitív progenitorok
4. Ngn3+ sejtek
5. PDMP (pancreas derived multipotent progenitor
6. β-sejtek

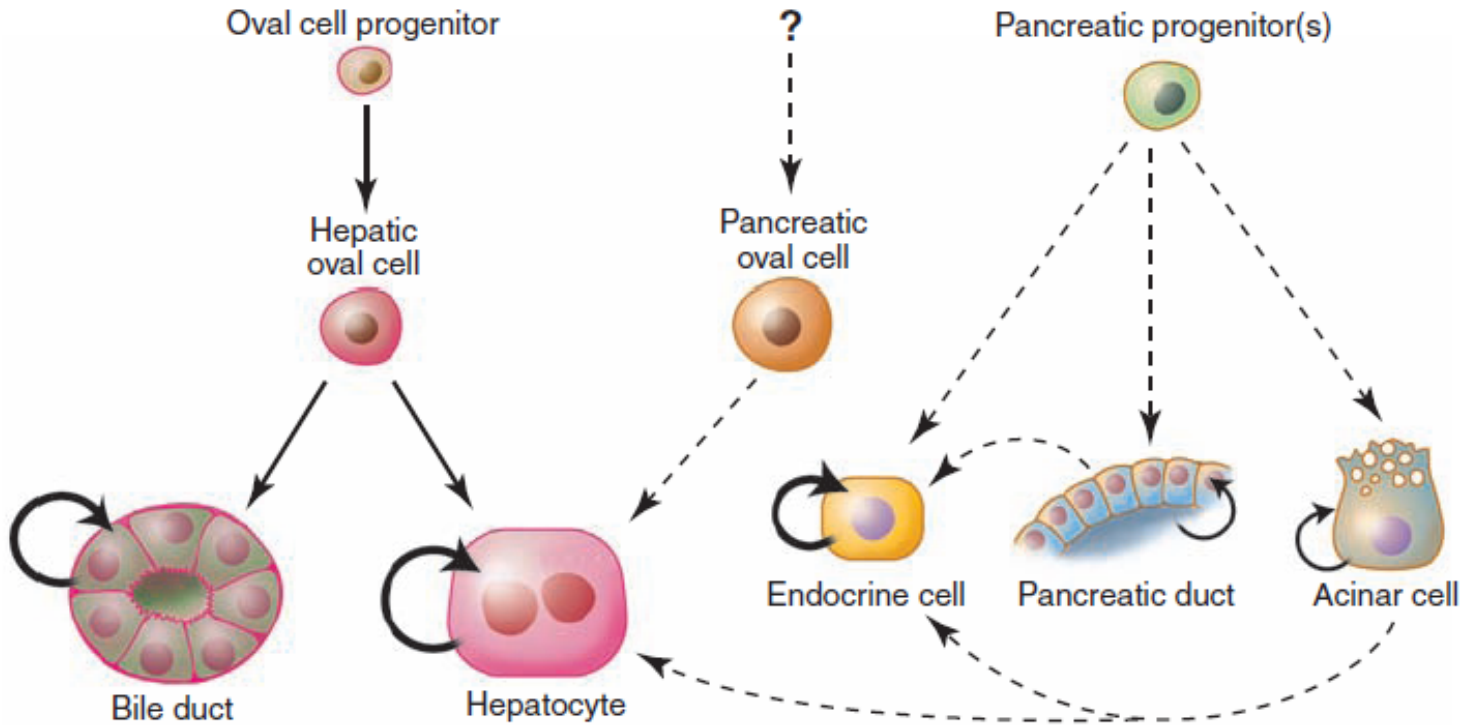

Fig. 4. Progenitor lineage relationships in adult liver and pancreas. The thickness of the arrows indicates the dominant mode of regeneration. Dashed lines delineate rare or hypothetical cell-fate transitions that occur only under specific experimental conditions.

Langerhans sziget transzplantáció

1980-as évek közepe: az első klinikai kísérletek
1990: az első hosszútávon sikeres átültetés (Univ. of Pittsburg)
1999-2004 között 471 beavatkozás 43 intézetben világszerte